

"Unraveling Rheumatoid Arthritis: Mechanisms, Management, and Future Frontiers"

Samina Mujawar, Vasim Aparadh, Vishakha Gurav, Saniya Mullani, Neha Gaikwad
Y.D.Mane Institute Of Pharmacy, Kagal.

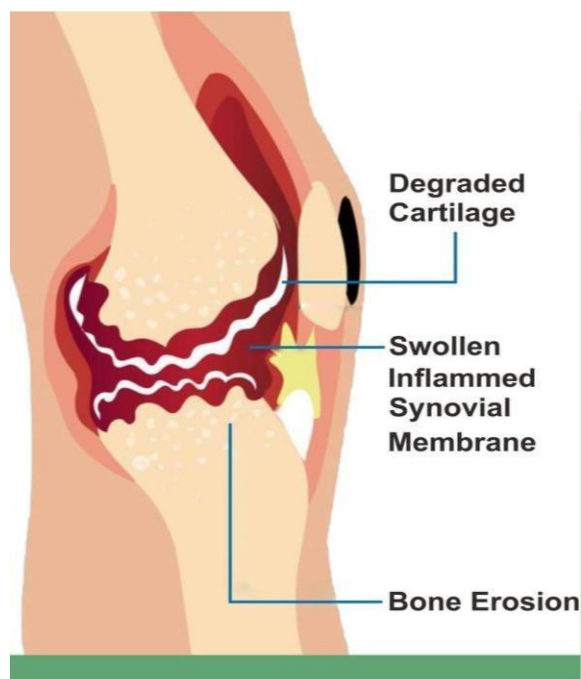
Abstract:

Rheumatoid arthritis (RA) is a chronic inflammatory disease characterized by joint destruction, bone and cartilage devastation, and rigidity, primarily affecting the elderly population and women. The disease is associated with an imbalance between autoimmune cells, resulting in systemic joint inflammation, chronic synovitis, and tissue destruction. With a prevalence of 1% in adults, RA ranks 42nd in terms of global disability and is linked to significant mortality rates, with 10-20% and 60-80% of deaths attributed to heart conditions and pulmonary problems, respectively. This review aims to provide an in-depth understanding of the molecular mechanisms underlying RA, including the role of major histocompatibility complex molecules and dependent T-cells. Furthermore, this study will examine the current treatment options and management strategies for RA, highlighting the need for a multi-faceted approach to mitigate the disease's systemic consequences and improve patient outcomes. By elucidating the complex interplay between autoimmune cells, inflammation, and tissue destruction, this research seeks to contribute to the development of effective therapeutic interventions for RA, ultimately reducing the burden of this debilitating disease on individuals and societies worldwide.

KEY WORDS: *Rheumatoid arthritis, arachidonic acid, synovium.*

I. INTRODUCTION

Rheumatoid arthritis is an enduring inflammatory disease that is categorized by bumping off the joint and rigidity, bone and cartilage devastation all above the joints. The disease is allied with the molecules of major histocompatibility complex, dependent T- Cells. This disease is more severe in the case of women rather than men and in the elder population [1]. The disease's results include systemic joint inflammation, chronic synovitis, and tissue destruction as a result of the imbalance between the autoimmune cells, which results in inflammation and cytokine release. The tissues will be harmed by the autoimmune antibodies [2]. In adults, rheumatoid arthritis affects 1% of the population. According to the primary cytology of comprehensive, this illness ranks 42nd. weakness. Death rates from rheumatoid arthritis-related heart conditions and pulmonary problems are 10–20% and 60–80%, respectively [3]. At present, individuals suffering from rheumatoid arthritis face concurrent events linked to a heightened cancer risk during or following treatment [4]. In the 1970s, the diagnosis of rheumatoid arthritis was made by examining the synovial fluid from patients, which revealed increased levels of prostaglandins. Various metabolites derived from the arachidonic acid pathway contribute to the depletion of both bone and cartilage.



The Stages of Rheumatoid Arthritis

STAGE 1

The body mistakenly attacks its own joint tissue.

STAGE 2

The body makes the antibodies and the joints start swelling up.

STAGE 3

The joints start becoming bent and deformed, the fingers become crooked. These misshapen joints can press on the nerves and can cause nerve pain as well.

STAGE 4

If not treated, the disease will progress to the last stage, in which there's no joint remaining at all and the joint is essentially fused.

FIG.1 These arachidonic acid metabolites lead to the inflammation of the synovium, which subsequently inhibits cell proliferation. Cyclooxygenases generate two isoforms, specifically COX-1 and COX-2, with COX-2 being primarily induced in inflammatory conditions and showing higher expression levels in the synovial tissues of individuals suffering from rheumatoid arthritis. (5) The reduction in the enlarged synovitis and the control of joint damage is noted with the administration of disease-modifying anti-rheumatic medications such as methotrexate [6]. Alternative medications for managing rheumatoid arthritis include dexamethasone (a glucocorticoid) and lornoxicam (a non-steroidal anti-inflammatory drug). (5) Recent advancements have led to the selection of new treatment options for rheumatoid arthritis. Biological agents that demonstrate significant pharmacological effectiveness with fewer side effects are now being favored. The main hurdles in developing and utilizing biological treatments are their stability and high costs. Given the elevated risk of adverse effects associated with synthetic medications, there is a growing interest in natural or herbal remedies. Several natural compounds with anti-rheumatic properties include brazilin, β -element, cardamonin, bufalin, celastrol, curcumin, and isogarcinol, among others. [7] The impairment of the joint occurs due to the complex interactions of immune modulators. During the progression of rheumatoid arthritis, various cells such as B cells, T cells, and macrophages (synoviocytes) play significant roles in advancing immunological responses. B cells enhance the inflammatory process by generating autoantibodies, such as rheumatoid factor and anti-citrullinated protein antibodies. T cells activate macrophages, which leads to the excessive production of inflammatory cytokines, including TNF- α , IL-1b, IL-6. The increased production of T and B cells will lead to the generation of cytokines and chemokines, resulting in heightened interactions among T cells, B cells, and macrophages. Inflammatory cytokines will encourage synovial cells to release tissue-destructive matrix metalloproteinases. Bone loss is driven by the activation of osteoclasts through TNF- α (8).

The word "arthritis" refers to a group of inflammatory diseases that impact the bones, muscles, and joints of the body. Joint stiffness, pain, redness, and swelling can be caused by a variety of arthritis types, including psoriatic arthritis, juvenile arthritis, gouty arthritis, osteoarthritis (OA), and rheumatoid arthritis (RA) [9]. An estimated 3 to 6 million people (15 percent) have arthritis, with 17 to 9 percent of women and 12 to 1 percent of men affected, according to (10). Furthermore, osteoarthritis accounted for 62% of patients with arthritis, rheumatoid arthritis for 12.7 percent, and an unspecified form of arthritis for 32.1 percent. In Australia, arthritis affects one in seven people (11). As people age, arthritis becomes more common and primarily affects women (ABS, 2017). Additionally, rheumatoid arthritis (RA) patients have a higher mortality risk than the general population [12], [13].

Rheumatic diseases are chronic and fluctuating in nature, with complex and unclear etiology, which further complicates the treatment of this type of arthritis [14], [15], [13]. However, even from the invention of various biological and synthetic treatments for RA, the decline in disease progression is achieved only in a small subset of patients [16], [17]. Furthermore, clinical trials for another rheumatic disease, Osteoarthritis (OA), are not very successful because of different disease phenotypes involved in the disease. Therefore, early diagnosis of the disease can slow its progression, where diagnosis involves many imaging techniques, including X-rays,

MRI and CT. However, diagnosis techniques, such as Kellgren Lawrence (KL) grade, are subjective, because their accuracy is largely dependent on the practitioner's experience [18]. Details of Kellgren and Lawrence's completion grading are given in Table 1. Computer-aided analysis and predictive modelling are necessary to overcome human error and for early disease detection in locations with fewer experts available, making the diagnosis process more methodical and dependable. Furthermore, a data-intensive study is necessary to develop a suitable treatment for arthritis, and artificial intelligence (AI) can be very helpful in identifying the condition. The sole goal of machine learning (ML), a branch of artificial intelligence, is to create data-driven predictive models that can learn from experience independent of the rules that people specifically specify [16]. In order to uncover hidden associations in data and create prescriptive, descriptive, and predictive tools to take advantage of these associations, it employs techniques, algorithms, and procedures [19]. Effective data representations can be automatically learned by machine learning algorithms [20], [21]. They are capable of handling a wide range of data inputs, including text and genetic data. G. medical imaging, patient cohorts, and electronic health records.

Additionally, it can produce results by identifying disease patterns and characteristics and learnin

from the information provided by clinical data. Additionally, it can aid in the optimization of treatment plans. As a result, it is clear that machine learning has greatly aided in bridging the gap in automatic learning from clinical experience. Additionally, deep learning (DL), a branch of machine learning (ML), makes use of big data, multi-layered neural networks, and computationally demanding algorithms [16], [22]. Both ML and DL have been applied to medical imaging over the past ten years, and it has been suggested that ML-based decision-making is better than doctors' individual clinical trial judgments [16]. Motivated by the latest commercial. This paper offers an overview of deep learning and conventional machine learning methods for the diagnosis of osteoarthritis and rheumatoid arthritis, motivated by the recent introduction of artificial intelligence in the medical field. Finding the present difficulties and unresolved research issues in this field is another goal of the paper. The current review papers [16], [23], [24], and [25] primarily concentrate on one particular type of arthritis. G. OA or RA and machine learning approaches exclusively, this study examines deep learning and machine learning approaches for diagnosing both OA and RA. Furthermore, Section 4point 2 of this paper offers comprehensive details regarding the publicly accessible datasets for RA and OA research. Our survey paper differs from the current review articles because of this. This is how the remainder of the paper is structured. The most prevalent forms of arthritis are covered in Section 2. Section 3 provides an overview of the most widely used machine and deep learning methods. A questionnaire. Sections 5 and 6 present machine learning and deep learning methods for arthritis diagnosis, respectively. Some of the unresolved research issues and challenges are covered in Section 7. Section 8 concludes the paper.

II. ARTHRITIS AND ITS TYPES :

One degenerative condition that affects human joints and can cause impairment is arthritis. There are several different kinds of arthritis, including juvenile, rheumatoid, and osteoarthritis., Psoriatic arthritis, gout arthritis, and arthritis. We shall go over rheumatoid arthritis, osteoarthritis, and psoriatic arthritis in brief in the sections that follow.

II.1. Rheumatoid Arthritis:

An autoimmune inflammatory disease that affects one or more joints and numerous organs is called rheumatoid arthritis (RA) [36]. A mix of environmental and genetic variables contribute to this disease's unknown etiology. The onset and course of disease are influenced by the complex interactions between these variables [37]. In general, RA is classified by morning joint stiffness and inflammation, which calls for expertise and experience to accurately diagnose the condition. The American College of Rheumatology (ACR) established a criterion for rheumatoid arthritis diagnosis in 1987 based on morning joint stiffness and edema, although this was not suitable for early disease analysis. Later in 2010, ACR/EULAR proposed a new criterion to make an early prediction of rheumatic patients[37]. as early detection and treatment of rheumatoid arthritis can slow down the disease progression and also increase the chances of cure.

II.2 Osteoarthritis:

(OA) is among the most prevalent musculoskeletal disorders, often leading to considerable disability in affected individuals. Knee OA is identified as the 11th leading cause of disability globally [38]. OA is characterized by the deterioration of articular cartilage, which is a smooth, resilient layer that facilitates seamless movement of the knee joints. In OA, the cartilage deteriorates, loses its elasticity, and becomes weakened [39]. Typically, it impacts the joints in the knee, hip, spine, and feet. According to [40], OA may arise from genetic predispositions or age-related factors. Additionally, it can manifest in younger individuals due to injuries, diabetes,

obesity, athletic activities, or in patients with rheumatoid arthritis. The main symptoms of OA encompass joint pain, difficulties in joint movement, and stiffness in the joints, particularly in the morning or after prolonged periods of inactivity [41]. Often, due to its ambiguous etiology, OA is not diagnosed until later stages, which complicates effective treatment, and in some cases, necessitates costly and invasive joint replacement surgery [38]. Nevertheless, early identification of the condition can help mitigate its progression. The current assessment of OA relies on a combination of clinical evaluations, symptoms, and radiographic techniques such as X-ray, MRI, and CT scans as needed [42]. Among the various proposed diagnostic methods for OA, the Kellgren-Lawrence (KL) grading system is recognized as the gold standard for classifying individual joints into five grades based on the severity of OA [39].

III.3 Psoriatic arthritis :

Psoriatic arthritis is a form of arthritis that impacts individuals with psoriasis — a condition characterized by red skin patches topped with silvery scales. Typically, individuals develop psoriasis initially and are later diagnosed with psoriatic arthritis; however, in some cases, joint issues may arise prior to the appearance of skin patches. The primary signs and symptoms of psoriatic arthritis include joint pain, stiffness, and swelling. This condition can affect any area of the body, including the fingertips and the spine, and its severity can vary from relatively mild to quite serious [43]. In this paper, we will concentrate on Rheumatoid Arthritis and Osteoarthritis, which are the most prevalent forms of arthritis and chronic diseases [44].

III. ETIOLOGY.

The etiology of rheumatoid arthritis is uncertain. It's possible that a genetically vulnerable host's reaction has changed. An infectious agent. The causative agents could be Mycoplasma, CMV, Epstein-Barr virus, rubella virus, and parvovirus. It is unclear how the infectious pathogen that causes chronic inflammatory arthritis spreads.

Factors influencing rheumatoid arthritis include :

- 1)genetics, 2)environmental factors, 3)smoking,
- 4) human micro biome

III.1 Genetic and environmental factors:

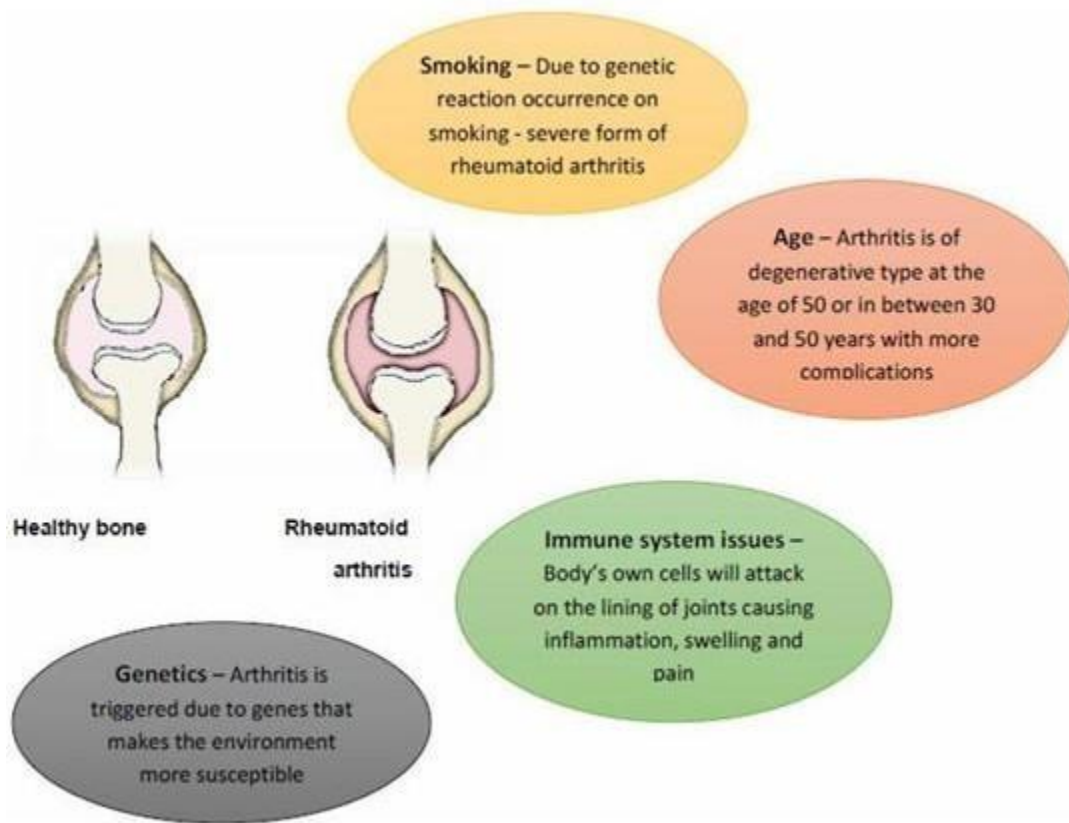
Rheumatoid arthritis has a genetic effect of 30% to 60%, according to several studies. Rheumatoid arthritis is mostly linked to the "shared epitope" found in the DRB1 allele. The presence of a common epitope increases the risk of rheumatoid arthritis by thrice.

III.2 Smoking:

Smoking is the main risk factor for the development of many chronic diseases. According to a few cohorts, the risk for the development of rheumatoid arthritis is more in ACPA-positive individuals who consume coffee. The relative risk factor is 2.06 with people who consume more than four cups of coffee. A Swedish cohort says that work-related exposure to mineral oil is the risk factor in men. The Swedish population whose profession is to work in mineral oil resources showed a 57% increase in the occurrence of rheumatoid arthritis. APCA positive individuals will develop rheumatoid arthritis in case of work exposure to silica. Other factors include lesser consumption of vitamin D and antioxidants and much more intake of sugar, sodium, red meats, proteins and iron which showed an increased risk of rheumatoid arthritis.

III.3 Human microbiome:

The transition from a symbiotic to a dysbiotic microbiome increases the likelihood of developing rheumatoid arthritis due to excessive microbial proliferation and a shortage of bacteria/organisms. This can lead to abnormalities in both innate and adaptive immunity [45].



IV. SIGNS AND SYMPTOMS:

With some regional variation, about 1% of the global population is impacted by An inflammatory condition. Native Americans, such as Chippewa Indians, have a higher prevalence of this disease (~6%), while Japanese, Chinese, and Saharan Black people have lower rates. Rheumatoid arthritis affects the wrists, fingers, feet, elbows, ankles, and knees in addition to the shoulders, hips, and cervical spine. Passive movement pain, swelling, heat sensation, and hardness in the mornings that lasts more than an hour are all signs of the illness. Fingers that resemble spindles are frequently seen. Rheumatoid arthritis is diagnosed when any of the aforementioned symptoms persist for more than six weeks.

Rheumatoid nodules, which are extravascular indicators, are frequently used to show rheumatoid arthritis. A radiating palisade and white blood cells On the stretching surfaces of the fingers and elbows, the hypodermis contains a central necrotic core of connective tissue. Other body areas such as the scalp, back, hands, feet, buttocks, or knees, heart valves, pericardium, lung parenchyma, and spleen are frequently found to have nodules.

Myocardial infarction, stroke, Raynaud's phenomenon, and infrequently, skin ulcers, are caused by vascular insufficiency in the peripheral region, which is brought on by blood vessel thrombosis. Lethargy, melancholy, thinness, lymphitis, clinical depression, aberrant splenic enlargement, muscle weakness, white nails, accelerated heartbeat, and fever (of unclear cause) are all systemic signs of rheumatoid arthritis.[118]

V. PATHOPHYSIOLOGY OF RA:

-Micro vascular injury appears to be the cause of the earliest abrasions in rheumatoid synovitis, and the increase in synovial lining cells (seen laterally with mononuclear cell infiltration in the perimysium).

- Under a microscope, the synovial lining's cells exhibit hyperplasia and hypertrophy, among other distinctive characteristics.

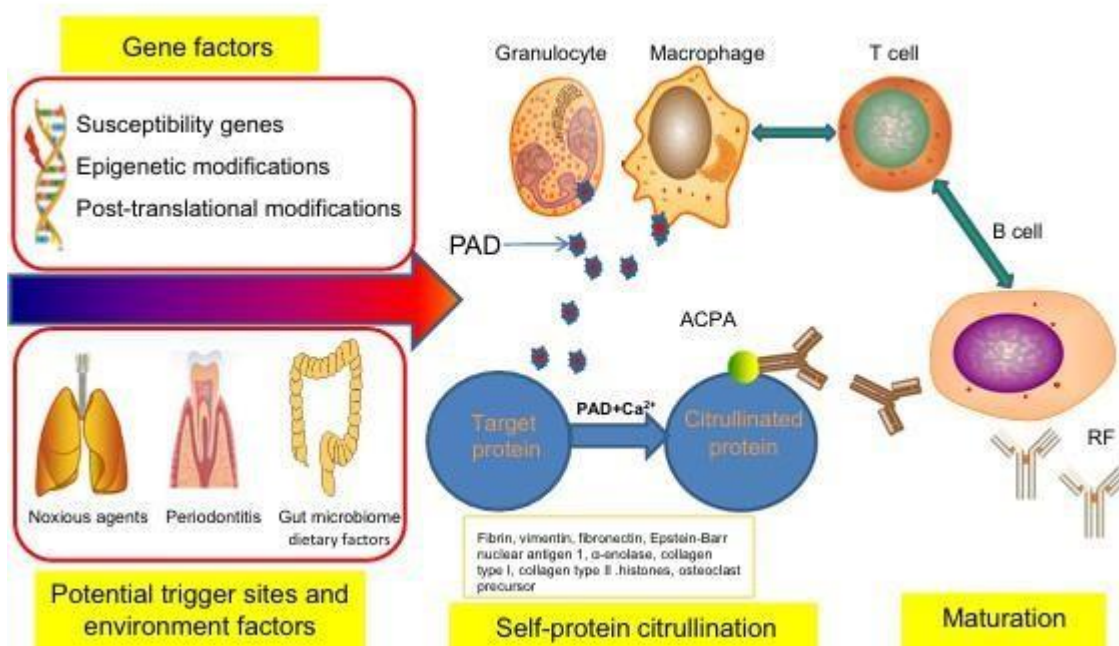
-The main or sectional variations in the vascular changes (includes embolism, ventricular damage and the development of new blood vessels where there is an impaired supply of blood in the region of trauma), dropsy and penetration with mononuclear cells (lymphocytes, monocytes, and immature granulocytes). High endothelial venules of lymphoid organs are seen in the endothelial cell

of rheumatoid synovium. This is changed when cytokines are exposed to enhance cell penetration into tissues, which leads to the steadily increasing number of linking molecules (participating in this process).

- The collections may differ in terms of the mononuclear cells' size and makeup. T lymphocytes are the main penetrating cells. These rheumatoid synovial cells are made up of CD4+ memory T cells, which aggregate to form the bulk of cells in the post capillary veins scattered throughout the body. T cells that are CD8+ are found throughout the tissues

-Despite the proliferation of T cells, rheumatoid synovitis is typified by the infiltration of many B cells and plasma cells that generate antibodies. The production of polyclonal Ig and autoantibody (rheumatoid factor) within the synovial tissue results in the local formation of immune complexes. The rheumatoid synovium showed an increase in the number of mast cells in their activated state, which causes local inflammation by releasing a little amount of material from their granules.

- The production of several enzymes (such as collagenase and cathepsins) by the synovial fibroblasts is clearly visible and will break down the components of the articular matrix. [109]Osteoclasts are the primary location of bone degradation. Trigger site of arthritis shown in fig.



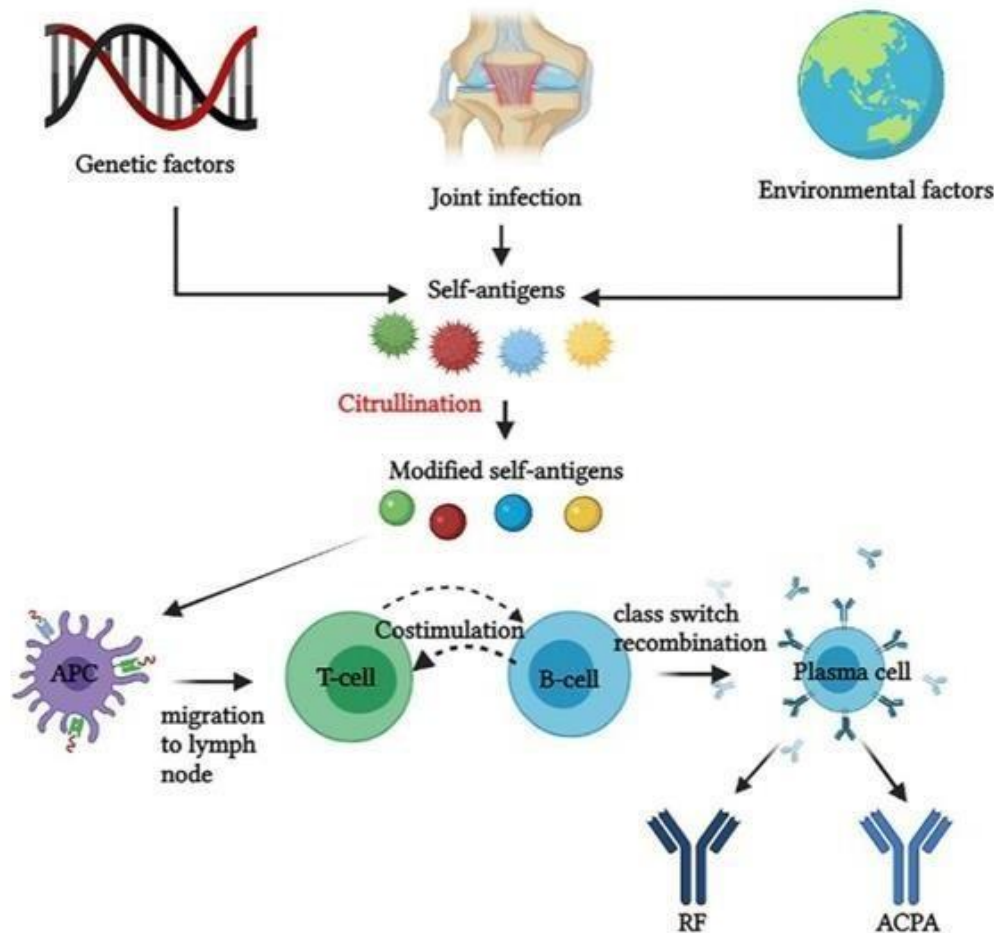
V.1 process in Pre-RA phase:

Although the fact that the pathophysiological mechanisms behind RA remain incompletely understood, a number of theories have been proposed. According to reports, immunological processes can take place years before joint inflammation symptoms appear; this is known as pre-RA. stage [26]. Modified self-antigens, including as immunoglobulin G (IgG), type 2 collagen, and vimentin, might result from the interplay between environmental influences and epigenetic changes on the genomic structure. Citrullination is a post-translational alteration that occurs when peptidyl arginine deiminase transform these proteins with arginine residues into citrulline [27,28].

Furthermore, cytokine production from joint conditions such as synovial hyperplasia or infections can result in joint inflammation and altered self-antigens [29].

The immune system can no longer identify citrullinated proteins (vimentin, type II collagen, histones, fibrin, fibronectin, and Epstein-Barr nuclear antigen 1,-enolase) as self-structures because of the susceptibility genes HLA-DR1 and HLA-DR4 [30]. Antigen-presenting cells (APCs), which are activated dendritic cells that start an immune response, absorb antigens. The entire complex moves to the lymph node, where CD4+ helper T cell activation occurs. Additionally, B cells in the lymph node's germinal center are stimulated by sequential and reciprocal impulses with T cells, a process known as costimulation in immunology

The interplay between CD28 and CD80/86 is an example of costimulation [31,32]. At this stage, B cells start to divide and develop into plasma cells that generate autoantibodies based on somatic hyper mutation or class-switch recombination. on the progenitor cells' receptors [33]. Self-tissues and organs are unintentionally targeted by autoantibodies, which are proteins generated by an immune system that is unable to distinguish between self and non-self components. The most researched autoantibodies linked to RA include RF and ACPA. RF is an IgM antibody that targets the Fc part of IgG, also known as the constant region, and has an 85% testing specificity in RA patients [34]. Additionally, it combines with complement protein and IgG to produce an immunological complex that can move through synovial fluid. ACPA is, however, more closely associated with RA as it specifically targets citrullinated proteins. Following these binding interactions, immune complexes are created and accumulate in the synovial fluid [35]. A summary of all the characteristics of the immune response during the pre-RA phase can be found in Figure as shown in below



VI. OVERVIEW OF MACHINE LEARNING

Supervised and unsupervised learning are the two categories into which machine learning algorithms fall. When learning under guidance, the link between input variables, such as a collection of features, and output variables, which provide classes or labels, is sought after by the machine learning model. After that, it calculates a function that can forecast output value for a collection of input values that aren't labeled [61]. Thus, labelled data is used to train models in supervised learning. Conversely, unsupervised learning does not require class labels and can identify the underlying patterns and structure in data [61]. Unsupervised learning, thus, refers to learning using unlabeled data.

The most widely used supervised and unsupervised learning strategies, including deep learning approaches, are covered in the sections that follow.

Techniques under supervision

A. K-nearest neighbors:

An algorithm for supervised learning is K-nearest neighbors (KNN).

It is applied to regression as well as classification. K-closest samples from the training set are utilized to forecast a fresh sample [62]. Depending on whether it is used for regression or classification, the output changes correspondingly. The majority vote of the samples' neighbors determines the class that is most common among the k samples with the most similar features in k-NN classification [63]. The result of k-NN regression is an object's property value, or the average of its k nearest neighbors.

Vector machine support :

For classification tasks, SVM is a conventional supervised machine learning model. It is typically utilized in binary problems. However, it can also tackle multi-class issues with the aid of different kernels, including polynomial. Hyperplanes are used by SVM to divide training data into distinct categories for classification. Consequently, SVM can be applied as a model that can categorize more recent samples [62]. Using various function weights, such as polynomial, SVM is trained to determine the most likely separation of discrete categories [63].

Decision trees

Decision trees are models that resemble trees and are made up of choices and the probable outcomes of those choices [63]. Unlike other machine learning techniques, decision trees combine feature gathering and classification operations into a single model [64].

Random forest

Compared to decision trees [63], random forest [65] is superior.

It is a machine learning ensemble classifier made out of several Regression tree classifiers and multiple local classifiers. It reduces bias and variance by classifying the input samples according to the majority votes of all the trees. It has been applied to choose the top-

performing models and rate the individual predictors [64]. The Random Forest technique aids in the reduction of associated variables and predictors. Crucially, the Random Forest can effectively handle correlation and interaction between variables thanks to the grouping property of sub-trees. Each tree in the Random Forest technique is created using two thirds of the data, with the remaining one third being used to identify misclassification. Although the Random Forest algorithm has identified a number of promising trees that are effective in choosing crucial indicators to identify patients However, whether RA or not, it is a "black-box" approach since it is challenging to comprehend the model's predictions and induce the explicit categorization rules [64].

Networks of artificial neurons

The computational models known as artificial neural networks (ANNs) are modeled after the biological nervous systems of humans and contain layers and contain components like neurons.

[66]. Classifying labeled data is one of the supervised learning tasks that ANNs are primarily employed for. Regression challenges can also be completed by artificial neural networks. Typically, an ANN has an input layer, output layer, and hidden layers. These layers are joined by varying weights and are made up of neurons [67]. It has been demonstrated that artificial neural networks outperform more conventional techniques like support vector machines and logistic regression.

B. Unsupervised methods

The most common autoencoder and other typical unsupervised learning techniques are covered in the sections that follow. and adversarial networks that are generative.

K-means grouping :

One method of unsupervised learning is K-means clustering [68].

This approach reduces the irregular separation space for each cluster by clustering the data into k clusters [69]. Depending on how far away the centroid is from nearby data, a centroid is chosen and categorization is accomplished [70].

Learning by reinforcement:

An unsupervised method called reinforcement learning is predicated on rewarding desired behaviors and/or penalizing undesirable ones.

ones [71]. An agent that can perceive and understand its surroundings, act, and learn via trial and error is the subject of reinforcement learning.

Reinforcement learning is a technique developed to reward desired behaviors and penalize undesirable ones. In order to motivate the agent, this approach gives desired behaviors positive values and undesirable behaviors negative values. This instructs the agent to look for the longest- term, highest total reward in order to arrive at the best possible solution. [71] .

C.Methods of deep learning

ANNs' capabilities are further enhanced by deep learning, which uses deep neural networks to map input data to the intended result [61]. Deep neural networks, which are made up of several successive layers and a number of fundamental non-linear operations called neurons, automatically learn the data representations in deep learning [63]. Different types of input data, such as text, medical pictures, or a combination of the two, can be processed by these systems. The performance of image processing techniques in particular has significantly increased with the use of deep neural networks [72]. Large-scale datasets like ImageNet have made it feasible to train data-hungry deep neural networks to identify and categorize a variety of pictures and items [73]. A deep neural network's structure differs from that of an artificial neural network (ANN) primarily in that it has multiple hidden layers [74].

The auto-encoder:

An encoder and a decoder are the two components that make up an Auto-Encoder (AE) [72]. The decoder and encoder both have hidden layers each, with the middle hidden layer serving as a shared third layer. The auto-encoder's encoder component determines a condensed, low- dimensional, meaningful representation of the input information. Combining the encoder and decoder and jointly training the encoder-decoder structure to reconstruct the input data by minimizing a cost function is how the encoder parameters are learned. Thus, the decoder can be described as a set of layers connected by a non-linear activation function that reconstructs the input from the output of the encoder.

Adversarial networks that generate

Goodfellow et al. initially presented Generative Adversarial Networks (GANs) [75] in 2014. The fundamental concept of a GAN is to have two neural network models in competition. The first model, known as the generator, creates samples by using noise as input.

Samples from both the generator (false data) and the training data (actual data) are fed into the other neural network, known as the discriminator, which distinguishes between the two sources [76]. These two networks go through an ongoing learning process in which the discriminator improves its ability to discern between produced and real data, and the generator learns to produce more realistic samples.

Both of these networks go through an ongoing learning process in which the generator gains the ability to generate more realistic samples and the discriminator gains proficiency in differentiating between created and actual data. With the goal of making the produced samples indistinguishable from actual data, these two networks are trained concurrently. The ability of GANs to back-propagate the gradient information from the discriminator back to the generator network is one of their benefits. Thus, the generator is able to modify its parameters to provide output data that can deceive the discriminator.

Neural networks with convolutions

Unlike conventional ANNs, convolutional neural networks are typically employed for pattern recognition [74]. CNN fraud consists of pooling and convolutional layers to create feature maps and learn features specific to images [76]. Compared to traditional ANNs, CNNs have demonstrated significantly improved outcomes for computer vision applications [74].

For the majority of image recognition, classification, and detection applications, the convolutional neural network architecture is widely used. It has been used to help individuals with musculoskeletal disorders (RMDs) and rheumatism. CNNs have been employed by researchers to identify bone erosions. Doppler ultrasound pictures have been utilized to measure the synovitis disease using similar networks. One problem with DCNN is that they need enormous quantities of training data and precise training parameters tuning [77].

A network with full convolution

To segment images semantically, a fully convolutional network (FCN) has been created. An enhanced model is FCN.in contrast to earlier architectures. It expands the classification capabilities of contemporary convolutional networks for segmentation and makes use of multiresolution layer combinations. It has been reported that FCN is effective and achieves high accuracy. FCN needs supervised pre-training and makes predictions at the pixel level. To accomplish the segmentation tasks, FCN can be constructed by converting many deep neural networks, including AlexNet, VGG net, and GoogleNet, into fully convolutional networks. [78]

U-net

Medical image segmentation is the primary application for U-net architecture. Compared to other segmentation methods, it contains less parameters. architectures. A network receives an entire image as input, and a set of trainable weights is used to produce matching segmentation masks.

[79] has shown that for image localization tasks, bounding boxes produced by U-net perform better than template matching techniques.

RetinaNet

Another well-liked architecture that has been applied to joint localization is RetinaNet. It is quite effective at setting the boundary. bounding boxes precisely to identify joints [80]. The foreground and background imbalance issue was not well addressed by earlier methods, thus RetinaNet was created to remedy it.

Using dense detectors, RetinaNet tackled the problem of severe foreground and background imbalance. To address the imbalance problem, the RetinaNet employs a unique focal loss technique. High precision and reduced computing time were the outcomes of this [81].

Even while deep neural networks produce highly accurate results, it's crucial to generalize these models to prevent over fitting, one of the main problems. Consequently, adjusting the The generalizability model is crucial. Furthermore, deep neural networks may be viewed as a mystery, leading medical professionals to doubt their methods and dependability.

VI.1 Imaging techniques and arthritis data:

This section's first section provides a quick overview of the imaging methods frequently used to diagnose RA and OA. After that, we'll talk about arthritic data that has been utilized in the literature. and the datasets that are openly accessible.

2.1. Imaging methods :

Rheumatoid arthritis (RA) and osteoarthritis (OA) can be diagnosed using a variety of imaging modalities, including computer tomography (CT), magnetic resonance imaging (MRI), ultrasonography, and plain radiography (X-ray images). The following is a quick discussion of several imaging methods.

X-ray :

Since X-ray imaging is non-invasive, it is the most extensively available and utilized technique for diagnosing osteoarthritis in the knee. It is imaging technique that is relatively quick, cheap, and simple to evaluate in order to track the progression of the disease [84]. Additionally, early- stage changes in bone structure can be reflected by X-ray imaging [82].

computed tomography :

An organ's CT is a three-dimensional volume image. It is the approach that is most frequently employed to visualize the human body. The drawbacks of CT include the administration of contrast agents and exposure to high levels of ionizing radiation [83].

Imaging using magnetic resonance (MRI) :

A common and appropriate method for diagnosing rheumatoid arthritis is non-invasive magnetic resonance imaging [85]. It provides a precise identification of the main pathophysiologic symptoms, such as myocarditis, vasculitis, and macro-/microcoronary artery disease, that affect the myocardium of people with RA [83]. For patients with retained metallic medical prosthesis, this imaging modality's drawback is that it is costly and ineffective.

PET scanning (positron emission tomography) :

PET uses radioactive material as a nuclear imaging method. Usually, it is absorbed in areas where inflammation is active and enhances the target lesion's visibility [83]. This technique enables precise volume measurement and blood flow measurements and perceives acceptance of positron-emitting radiotracers. Ionizing radiation and high cost are among its drawbacks [85].

Carotid ultrasound (CUS)

At the moment, CUS is the most reliable non-invasive method for providing the most thorough and validated evaluations of development. expression of RA. Additionally, it is an affordable imaging technique that provides RA patients with early illness information.

Data and databases related to arthritis:

Rheumatoid arthritis :Given that arthritis is a condition that impacts several parts of the body parts like the knee, hands, and hips, the technique used to acquire the data, and The origins of popular datasets differ greatly from one another. First off, a number of research have attempted to comprehend RA, but they have consistently depended on one or a small number of hospital data to accomplish their goals. Kim et al., [86] identified persons with rheumatoid arthritis by looking through medical records. Out of 9,482 patients, only 2% replied and gave their permission for their medical records to be reviewed. Clinical data was used in research conducted by Yoo et al. [70] and Lezcano-Valverde et al. [87]. 60 patients from Euji University Hospital provided data for the first method, while 280 records from the Universitario de La Princesa Early Arthritis Register and 1461 records from Hospital Clinics San Carlos were used for the second. Longitudinal study dataset for Rheumatoid Arthritis patients.

Although Murakami et al. [88] used hand radiographs chosen by skilled radiologists, the study only included 159 instances overall, 30 of which were used to validate the Deep Convolutional Neural Network. Three different synovial subtypes were identified by Orange et al. [89] using the synovial gene signatures of RA patients. A histologic grading method was created using these markers, and the histologic scores connected with clinical metrics like C-reactive protein (CRP) level and ESR. The 500 most variable genes were chosen by the authors from 45 synovial samples (from 39 RA and 6 OA patients) and 14 histologic features from 129 synovial samples (from 123 RA and 6 OA patients).45 synovial samples (from six OA patients and 39 RA patients) contained nes. K-means clustering, which divides n items into k groups, with each object belonging to the cluster with the closest mean, was used to investigate gene-expression- driven subgrouping. The most reliable clustering at 3, and although not in a separate dataset, principal component analysis was used to corroborate this subgrouping. Based on their gene patterns and enriched ontology, three groupings were identified: high-inflammatory, low- inflammatory, and mixed subtypes. In order to provide a practical histology-based method for characterizing synovial tissue, the study sought to ascertain the synchronization between synovial histologic characteristics and genetic subtype. A leave-one-out cross-validation SVM classifier was used to achieve this. Finding a decision hyperplane that divides data points of various classes with a maximal margin—that is, the maximum distance to the closest training data points—is the goal of an SVM. The effectiveness of the model in distinguishing between the The evaluation dataset for the high and low inflammatory subtypes was minimal, which led to SVM overfitting, while the other subtypes were comparatively good .

A limited number of patients have been the subject of analysis in other research. For example, 60 anonymous patients' numerical data was used by Singh et al. [90]. Additionally, Ureten and colleagues [91] utilized datasets from two hospitals, one of which is utilized for testing, while the other was utilized for training. This additional information aided in understanding the research's applicability and validity. The UH and SNH Cohorts provided the data, respectively.

Furthermore, a number of research began using medical imaging data for analysis. For example,

[91] used radiographs from the medical faculty's outpatient clinic, and 50 used ultrasounds, which included 1342 Doppler ,US images.

The clinical data was examined by Yoo et al. [69] in order to predict RA. Euji University Hospital provided the data for the study, which involved 60 RA patients. This study discovered that the standard RA diagnosis criteria suggested by the American College of Rheumatology (ACR), was inadequate for the disease's early identification when it was first created in 1987. Rheumatoid factor (RF), anti-CCP, SJC, and ESR clinical data were therefore used to assist rheumatologists in making early predictions. Using k-means clustering, the patient data was examined to determine the threshold values for four factors: RA factor (RF) >7, Anti CCP >18, SJ >4, and ESR >25. These factors were used to predict RA. The study found that 84% accuracy was attained for K=4. Furthermore, choosing two criteria and determining their correlation is more effective than choosing just one parameter. According to the K-means algorithm, two of these four factors can indicate RA, and rheumatic disease may develop if one of the two factors—RF and AC—is positive.

Osteoarthritis :

Since the issue with osteoarthritis differs from that with rheumatoid arthritis, different kinds of data are gathered, processed, and analyzed. Much progress has been made because the existence of openly accessible imaging databases like MOST (Multicentre Osteoarthritis Study) and OAI (The Osteoarthritis Initiative). Deep neural network testing and training are made possible by these datasets. 500 of the 4796 participants in the OAI dataset were used for performance testing by Thomson et al. [92]. Additionally,

Antony et al. used X-ray images from the OAI dataset in 2016 to assess their method on 4,476 pictures.

Some research, such Gornale et al. [93], [94], have only employed 200 and 207 knee X-ray images for training and testing, respectively, and have used smaller datasets. A total of 616 X-ray pictures from different hospitals were used by Gornale et al. [95]. Tiulpin et al. [96] obtained 1574, 93, and 77 knee radiographs, respectively, from a variety of sources, including MOST, Central Finland Centre Hospital, and OKOA. A small number of previous research, including those by Antony et al. [99], Tiulpin et al. [97], and Tiulpin et al. [98], have combined the OAI and MOST datasets, dividing them into test and training sets. This made it easier to assess if their suggested framework could manage large amounts of data and be used with general populations.

Additionally, a small number of research, including Tolpadi et al., [100], began using MRIs because of the benefits of 3D pictures. They employed 4,796 patients' 2D radiography and 3D MRI images to achieve high performance using three-dimensional CNNs. TSE and DESS images from 718 case-control patients (274 males and 444 females) were used by Wang et al. [101].

Yoo et al., [70] used KNHANES V-1, and bilateral radiographs were retrieved for participants who are over the age of 50. There were 2665 participants in the study, and 4731 persons from the OAI dataset were externally validated. Liu et al., [82] used a dataset collected at a hospital in Shanghai that consisted of 2,770 X-ray images. Von et al., [80] used 15,364 hip joint scans to model the severity of hip osteoarthritis.

VI.2 Machine learning for the diagnosis of arthritis

Finding joints in pictures like X-rays, MRIs, and CT scans is a significant and difficult step in the automatic diagnosis of arthritis. Here, we examine some of the most recent ML methods for arthritis diagnosis are used for joint detection techniques

ML techniques for joint detection

A template matching technique was presented by Shamir et al. [102] to identify the knee joint center in a 20x20 pixel picture patch. Their method involved downscaling the x-ray image to 10% of the real image size, after which it is subjected to histogram equalization in order to normalize the intensity. The Euclidean distance was then determined by scanning each input image through a 20x20 sliding window. The knee joint center was identified as the window with the minimum Euclidean distance. The technique was simple to use, but for large data, it was slow and had poor detection accuracy [99].

Fully convolutional n(99) was employed in the study by [103]. Based on the mean aspect ratio (1.6), the input image's size was chosen to be 200 x 300 in order to maintain the aspect ratio. for every region of interest that was extracted. Using knee X-ray scans, they assigned a severity rating to the impairments based on the Kellgren and Lawrence criterion, which is a five-point ordinal scale. Using clinical evaluation data from patients, prediction models were constructed using the Random Forest (RF) and Elastic Net (EN) methodologies.

Employing YOLOv2 for knee detection, [104] maintained the initial knee joint size close to the real knee joint size, which was determined by clustering on all the available knee joint training. Object detection in YOLOv2 is viewed as a regression issue that improves height, width, and center coordinates for each bounding box situated in each grid center, along with the confidence score. According to their experimental findings, YOLOv2 outperformed HOG-SVM [96] and FCN [105].

To locate knee joints, Norman et al. [79] used the U-net model. In order to pre-process the x-ray radiographs, the image was divided in the middle, followed by the left and right knees.

The image's side was inverted. Next, bounding boxes around the knee (about 500 photos) were created using a 2-D cross-correlation template approach. After that, these 500 bounding boxes were examined to make sure the template accurately extracted the knee joint region.

Furthermore, the U-net network was trained using 450 images of the localized knee joints. After that, the model's output was manually confirmed using a fresh dataset of 500 knee photos.

According to their experimental findings, the knee was accurately localized by the bounding boxes produced by U-net. For 1000 randomly selected examples, U-net's accuracy of 98.3% showed improvement above the baseline template matching method. Next, they used radiography and deep learning to forecast severity of OA. It's interesting to note that the authors combined KL grades 0 and 1 because they thought the clinical response was the same for both.

A regression-based deep learning technique was put forth by Tiulpin et al. [98] to solve the problems associated with anatomical landmark localization in knee x-ray radiographs for various stages of osteoarthritis. The authors claim that landmark localization is broken down into two smaller tasks: self-localization of landmarks and region of interest (ROI) localization. The latter is used for bone shape and texture analysis, while the former is used for a thorough examination of knee pictures. Furthermore, manually annotating without knowledge of knee anatomy is a minor problem that gets more difficult as the severity of OA increases.

Additionally, they created the BoneFinder tool for annotations and performed annotations using the VGG image annotation tool. This method employed a soft-argmax layer to directly evaluate each landmark point and an hourglass convolutional network to locate landmarks

.Two separate datasets were used to assess the method's performance, and it outperformed the most advanced baseline technique Region proposal networks (RPNs) were used by Liu et al.

[82] to locate joints in the input X-ray images. Conventional object detection techniques often use computationally costly economic inference procedures and cheap characteristics. This bottleneck is removed by fully convolutional networks, which also produce high-quality region recommendations that fast R-CNN uses for object detection.

The network has 101 layers, with batch normalization and ReLU activation layers coming after each convolutional layer to prevent overfitting. Furthermore, the max-pooling and convolutional layers explain features and produce convolutional feature maps that are shared by Fast R-CNN and RPN. These feature maps are used as input by RPN to generate region recommendations as an output. After calculating each region's coordinates and RPN inferencing scores, non-maximal suppression (NMS) is used to eliminate redundancy during detection. The anchor box with the greatest RPN score was retained following the application of NMS. An end-to-end deep learning model for the diagnosis of osteoarthritis in the knee might be created using their suggested methodology.

Tolpadi et al. [100] predicted a patient's likelihood of needing a knee replacement during the next five years of their life using MRI images on DenseNet-121. The OAI dataset, which included both imaging and non-imaging variables, was used in the study. They pre-processed the radiographic MRI images using the same methodology as in [79] by limiting them to a 500x500 area in the knee joint's center. Next, the bounding box was identified using 2D cross-correlation template matching. They then trained a U-net architecture to recognize the OAI study's posteroanterior radiographs.

Similar to [98], Hoang et al. [106] employed a random forest regression voting constrained local model technique in the BoneFinder tool. Next, using cropped ROIs of 140 mm × 140 mm surrounding the knee joint picture and localized anatomical features they carried out the standardization of each ROI by horizontally aligning the tibial plateau (up to two ROIs per image). After images were flipped and broken up, intensities were finally normalized. In [105] and [97], input data was normalized using training set statistics. Nonetheless, the authors employed a 0.5 mean and a 0.5 standard deviation in their investigation

. RetinaNet was trained to identify the left and right hip joints in a radiograph in a recent study [80]. Additionally, the 640x640 input size image of a single hip was rescaled to 224x224 pixels, cropped, and contrast-stretched. A DenseNet pertained For the multitask neural network implementation, 161 functioned as a shared convolutional feature extractor with a multitask loss function. To achieve the final evaluation, each completely linked layer was trained for each radiographic characteristic of OA. The findings demonstrated that RetinaNet correctly positioned bounding boxes for each joint image, with an accuracy of 80.8%.

In a method put forth by Thomas et al. [107], the image was divided into left and right knee joints, and all of the dataset's images were reduced to 299 x 299 pixels to give the neural network model a consistent input. Since the resolution, pixel sizes, and scale of the original photos differed, two model architectures were first taken into consideration. In order for the created photos to match the distribution of images in the original dataset, the original images were cropped, zoomed in, up scaled, noised, flipped horizontally, and contrast changed throughout the image augmentation process. In addition to this, the training set images were replaced by numerous altered versions (for instance mirroring an image and alteration of contrast for converting a right knee of high contrast to a left knee of low contrast), a model was prepared to do predictions for new images with different parameters than those traced in original non augmented training set.

VII. ML TECHNIQUES FOR ARTHRITIS DIAGNOSIS:

Lezcano-Valverde et al., [87] demonstrated the use of machine learning method in the development and validation of a predictive model for rheumatoid arthritis mortality based on demographic and clinical variables. The drawbacks of conventional survival strategies, such as limited assumptions, proportional hazards, and parametric and non-linear factors that lead to overfitting, are addressed by the Random Survival Forests (RSF), a nonparametric technique. Using bootstrap sampling, the RSF approach builds a cumulative risks function and several decision trees. (CHF) from each individual tree, which are subsequently averaged to provide an ensemble CHF. In this investigation, two distinct datasets were employed. One comes from the 1,461 individuals in the Hospital Clinico San Carlos RA cohort (HCSCRAC). Rheumatologists use this daily clinical practice cohort to make a clinical diagnosis of RA. It is employed in the model's training process. . The other dataset comes from the 280 RA patients in the Hospital Universitario de La Princesa Early Arthritis Register Longitudinal (PEARL). It is employed in the validation of the model. The clinical and demographic factors were gathered over the initial two years of a RA diagnosis. In a follow-up period of 4.3 and 5 years, respectively, the mortality rates for HCSCRAC and PEARL were found to be 22.1% and 14.6%. Higher predictive capacity was demonstrated by characteristics like age at diagnosis, median erythrocyte sedimentation rate (ESR), and number of hospital hospitalizations. The training and validation cohorts had prediction errors of 0.187 and 0.233, respectively. In general, potential factors for mortality risk have been recognized. They achieved success in creating a forecasting model for RA mortality that has enabled the identification of subgroups at elevated risk of mortality. For additional research, outside Verification and targeted measures can be implemented to lessen the risks of mortality for the subgroups at elevated mortality risk.

Gornale et al., [108] suggested a computer-assisted evaluation of the knee.OA employs the active contour segmentation technique along with K-NN for its implementation. Categorize different calculated attributes. The dataset contains 207 knee X-ray images from individuals of varying ages, genders, and blood types. And jobs. In this study, image collection and preprocessing are conducted, succeeded by image segmentation, which is performed utilizing the Active Contour Segmentation technique (ChanSubsequently, image enhancement (Contrast Adjustment method) is executed to obtain a higher quality image. Subsequently,

different characteristics such as Shape characteristics, Statistical characteristics, First four moments, Haralick attributes, texture analysis characteristics and Zernike moments are calculated, and classification is executed. Utilizing the K-nearest neighbor classifier. The stated classification accuracy rate is 88.88%, and their method determines whether the provided image is either normal or impacted and Edge methods are employed).

Gornale et al., [94] developed a semi-automated approach for the identification of Knee OA. The dataset employed in their research includes 200 Knee X-ray images gathered from different hospitals according to age, sex, blood type and profession. In the suggested method, initial image collection and pre-processing take place first. The image is then segmented through Active Contour segmentation approach (Chan-Vese Edge techniques). Subsequent to that picture improvement The method (contrast enhancement) helps to enhance the picture. Caliber. Subsequently, different aspects including Haralick, Statistical, and First Four instances, Texture and Shape are calculated. These characteristics are additionally categorized with the Random Forest classifier. Based on authors, since solely radiological evaluation of knee X-ray has been taken into account for this study, hence, a rate of misclassification is noted when taking individuals into account. The accuracy rate of their method for classification is 87.92% when the features are combined. Jointly. In the future, it's necessary to take into account both clinical symptoms and radiographic evaluations to create a detection method. to improve the classification rate.

In a separate study, Gornale et al., [95] created a machine vision technique for diagnosing Knee OA through region-based and dynamic form model. The computation of features includes histograms. Of the histogram of oriented gradients (HOG) technique. The calculated gradients are categorized using a multiclass SVM classifier to analyze OA based on KL (Kellgren-Lawrence) grading scale. The dataset is made up of 616 digital knee X-ray images obtained from multiple hospitals and diagnostic centers based on various characteristics like age, gender, blood type, job and weight of patients. The pictures are of dimension 1345×2451 and DICOM Standard (Digital Imaging and Communications in Healthcare). Two renowned medical professionals assigned KL ratings to every Knee X-ray image. Initially, implicit active contour algorithm was used to preprocess and segment X-ray images. HOG features were obtained from these X-ray images for additional processing, and subsequently, those features were categorized. Employing SVM. The classification accuracy reached 97.96% for Grade-0 and 92.85% for Grade-1 achieved 86.20%, while Grades 2, 3, and 4 scored 100% respectively. The classification outcomes confirmed by the two Experts show a strong consensus with 94.96% and 94.64% respectively. Additionally, the suggested approach produced superior outcomes with 95% accuracy in comparison to techniques utilizing active contour. Segmentation to obtain ROI and Random Forest Classifier with recognition rate of 87.92% and K-NN Classifier for classification percentage of 88.88

Thomson et al. [92] carried out a Random Forest Regression. Voting Constrained Local Model (RFCLM) for identifying bone positions and for identifying the key landmarks surrounding the tibia and femur effectively. They merged characteristics from bone structure. And image texture in tibia derived from 500 X-ray scans and subsequently utilized two stochastic forests utilizing a weighted method.

Their documented findings indicated that the integration of form and texture-oriented models offer a considerable enhancement in overall classification performance improved as the accuracy measurement rose from 0.789 to 0.849 when employing both shape and texture instead of just the shape alone. Tiulpin et al., [96] employed the HOG feature descriptor for preprocessing and utilized a linear SVM that had been pre-trained on radiographic data. Images obtained from three sources (MOST dataset - 1,574 Images, Central Finland central hospital – 93 and OKOA - 77). The research presented a system that can be used for extensive analysis. Nonetheless, this study has one limitation. The images received annotations from a single individual and thus might exhibit a possible bias.

Furthermore Consequently, additional research on localization needs to be carried out. to enhance this approach Subramanian et al., [115] applied SVM with combined kernel functions to classify 130 radiographic images (30 normal and 100 abnormal) based on the Haralick features obtained from the ROI. one-dimensional information and inadequate for proper categorization. Thus, kernel functions (including linear, polynomial, and Radial basis functions were employed to transform the one-dimensional data into higher dimensions. Dimensional to enhance the effectiveness of classification. KL assessment A system was utilized to assess the Articular Space (AS) between bones, as the decrease in space suggests OA. Additionally, solely the Cases categorized as grade 0, grade 1, and grade 2 were taken into account, while the others were excluded. All were dismissed since joint space narrowing was readily foreseeable without employing any aiding instruments. In the classification process, the SVM classifier employed hyperplane classification to categorize extracted features. From ROI of knee joint into typical AS and atypical AS joints. The findings showed that improved classification results were achieved. Using RBF kernel functions. Additionally, the accuracy of the classification was enhanced by combining extracted features and sequential kernel functions%

VIII. DEEP LEARNING TECHNIQUES FOR ARTHRITIS DIAGNOSIS:

In addition to conventional machine learning methods, sophisticated Deep learning methods have also been applied for the diagnosis. Of joint inflammation. In the subsequent sections, we explore the pertinent deep learning methods. (Refer to Table as well.) Antony et al. [105] used Convolutional neural networks on Radiographs (4,476 Participants) for assessing Knee Severity utilizing Kellgren and Lawrence Classification. The classification outcomes utilizing features obtained from pre-trained CNNs (VGG16, VGG-M-

128 and BVLC Caffenet) demonstrated superior performance compared to OA classification. Table presents a summary (in sequential arrangement) of machine and deep learning methods for the identification of arthritis.

Reference	Year	Technique	Dataset size No.of patients or images	Modality
Thomson et al.,(92)	2015	RFRVCL/SVM	500 images X-ray	X-ray
Subramoniam et al.(115)	2015	SVM	130 images	Radiographs
Antony et al(105)	2016	CNN	4476 patients	MRI
Gornale (108)	2016	Active Contour Segmentation	200 images	X-ray
Gornale(94)	2016	KNN	207images	X-ray
Yoo(70)	2016	k-means	60 patients EHR	HER
Gornale et al.,(95)	2017	HoG/SVM	616 images X-ray	X-ray
Antony et al.,(99)	2017	FCN/CNN	7502 patients MRI	MRI
Lezcano-Valverde et al.,(87)	2017	Random Survival Forest	1741 patients	HER
Murakami et al.,(88)	2018	CNN	30 patients Radiographs	Radiograph
Tang et al., (116)	2018	CNN	-	Ultrasound
Orange et.al(89)	2018	SVM	129 Patients	Tissue samples
Norgeot et.al(110)	2019	LSTM	820 Patients	HER
Hemalatha et.al(117)	2019	CNN	-	Ultrasound
Abedin et.al(103)	2019	Elastic Net/Random Forest /CNN	4796 patients	MRI
Chen et.al(104)	2019	YOLOv2	-	X-ray
Tiulpin et.al(112)	2019	Reset Net-34	-	Radiographs
Norman et.a(79)	2019	U-Net	500 images	X-ray
Tiulpin et.al(98)	2019	Deep learning Regression	-	X-ray
Liu et.al(82)	2020	Fast RCNN	-	X-ray
Tolpadi et.al(112)	2020	DenseNet-121	-	
Hoang et. al (106)	2020	Forest Regession Voting	-	X-ray
Bonaretti et.al(113)	2020	Extended Phase Graph (EPG)	10 patients	
Dang et.al (118)	2020	CNN	200 patients	X-ray
Von et.al(80)	2020	RetinaNet	-	X-ray
Chen et.al(104)	2019	CNN	-	X-ray
Nguyen et.al(114)	2020	Siamese Network	500 images	X-ray

Utilizing an open-source tool for biological visual content examination. Additionally, characteristics from the conv4 layer and the pool5 layer of VGG-M-128 network and conv5 layer, pool5 layer from BVLC Caffenet achieved better classification accuracy compared to fully connected layers (fc6and fc7) of VGG networks and CaffeNet. Subsequently, classification with multiple classes Linear SVM was applied, and once more, CNN features surpassed the Wndchrn tool, with the classification accuracy of both convolutional and pooling layers exceeding that of the fully connected layer stratum. Along with that, BVLC CaffeNet and VGG-M-128 architectures were optimized by replacing the upper fully connected layer, which enhanced multi-class classification with refined BVLC achieved marginally superior results compared to VGG-M-128. Additionally, authors contended that considering KL grades as discrete variables may lead to classification problems and inaccurate predictions.

Consequently, they suggested additional suitable method to evaluate the severity of Knee OA performance by utilizing a continuous assessment metric like mean squared mistake. The BVLC CaffeNet model, which was pre-trained, underwent fine-tuning utilizing classification loss (cross-entropy applied to softmax outputs) and regression loss (mean squared error) for evaluating performance of evaluation of knee OA severity. The findings showed that it lowered both mean squared error and enhanced multi-class classification precision of the model. The MSE was notably reduced in the The loss for CNN regression is at 0.504, whereas the losses for CNN classification network and Wndchrm are 0.836 and 2.459, respectively To assess whether regression loss yields superior classification accuracy, the network trained with classification

Loss and trained with regression loss was also evaluated. It was noted that the multiclass classification precision of networks adjusted for regression the loss was 59.6%, while for classification loss, it stands at 43%. Thus, the network that was trained using regression outperformed the network trained using classification loss. This is due to the reality that regression offers additional insights to the network regarding the connections among KL grades and enables them to improve generalization for the unobserved data.

In a different study, Antony et al., [99] utilized the blend of FCN and CNN, with FCN applied for Knee Detection, while CNN was utilized for both classification (0, 1, 2, 3, 4) and regression (0 to 4) assignments to forecast the severity of the KL grade. The classification outcomes are contrasted with Wndchrm, and this model developed from Scratch surpassed Wndchrm with an accuracy of 60.3% and MSE.0.898. The outcomes are superior to those previously stated. methods employing BVLC CaffeNet for the classification of Knee OA X-rays via transfer learning. These enhancements result from the .The network features a lightweight architecture with fewer parameters (5.4 million) in contrast to the 62 million parameters of BVLC. When the the network is simultaneously trained for both classification and regression of the knee In the images, the learning curves indicate a reduction in training and validation losses, along with a rise in training and validation accuracies throughout the training process. Furthermore, an enhancement in the accuracy for multi-class classification was noted for the network together prepared for classification and regression in contrast to the earlier approach. The confusion matrix showed that the categorization Knee OA images conditioned on KL grade 1 presented issues due to minor variations.

Chen et al. [104] utilized two deep convolutional neural networks. (CNN) to evaluate the severity of knee OA automatically and utilized the Kellgren-Lawrence (KL) classification system. Initially, a tailored a single-stage YOLOv2 network was introduced for detecting knee joints, in X-ray images with minor differences. Secondly, the most favored CNN architectures such as ResNet, VGG, and DenseNet (various versions) along with InceptionV3 have been optimized for classifying the identified knee joint images. They additionally created new customizable ordinal loss function that enhanced the classification precision and lowered the MAE for all classification models. The dimensions of X-ray images of the knee are 2048×2560, which were quite substantial for YOLO version 2. Consequently, it was adjusted to the dimensions of 256×320 for all the radiographic images. The outcomes were achieved through the application of cross-entropy. Loss and the suggested ordinal loss. In every comparative classifier, The ordinal loss achieves higher accuracy and reduced MAE in knee joints that have been manually cropped. The majority of classifiers (excluding ResNet-152, VGG16bn, InceptionV3) achieve greater accuracy when detected automatically. Knee articulations

. All classifiers, nonetheless, achieve reduced MAE. These results demonstrate the greater effectiveness of a suggested ordinal loss function M. Imtiaz, S.A.A. Shah, and Z. ur Rehman Neuroscience Informatics 2 (2022) 100079 for knee KL grading. Certain classifiers, like ResNet- 101(MAE: 0.408, 0.391, accuracy: 65.5% and 66.7%) and VGG-16 (MAE:0.356, 0.358, precision: 68.5% and 69.1%), achieve even higher accuracy and reduced MAE for knee joints identified automatically. The optimized VGG-19 model attains the highest classification performance. For knee KL grading in comparison to the ResNet or DenseNet versions, confirming that the effectiveness of CNN models was greatly influenced by the training task. The VGG-19 model that has been fine-tuned with the suggested ordinal failure in the knee grading function achieves the highest classification accuracy of 69.7 percent and mean absolute mistake (MAE) of 0.344.

Norgeot et al., [110] introduced long short-term memory (LSTM) methodology for diagnosing and forecasting the development of rheumatic arthritis condition. In their research, the electronic health record (EHR) of patients was utilized to train and evaluate the LSTM. The data collection utilized in their research includes 820 patients.

Li et al. [111] employed Convolutional Siamese Neural networks to evaluate knee severity utilizing the KL grading scale. The research uses a finetune ResNet-34 as a reference point and presents innovations like creating a novel method that employs Siamese networks to decrease the trainable parameters and reducing the model's sensitivity to noise.The research successfully utilized radiographs from both MOST and OAI.data collections. Only the images with 5, 10, and 15-degree beam angles were utilized from the MOST dataset. To handle the images,instead of understanding images through the similarity metric among the pairs,the research utilized symmetry within the image and the network was capable of acquiring the same weights for image edges. The Siamese breed network successfully decreased the quantity of parameters that needed to be learned.

This assisted the model in limiting itself to aspects that a human specialist would concentrate on. The model reached a multiclass accuracy of 66.71% and AUC of 0.93 on the OAI dataset Nonetheless, the qualitative evaluation of the test set showed that the A fine-tuned model might acquire characteristics that are unhelpful or unrelated. The research additionally employed GradCAM to assess if the the model has been acquiring the appropriate characteristics. One of the largest Advantages of this method include that both the model and the results are replicated since the dataset and the implementation (code) are accessible to the public.

Tiulpin et al., [112] created a multimodal system to produce prediction output on the advancement of Osteoarthritis. The investigators suggested frameworks for the pipeline that can accept the input from unprocessed images to produce outcomes. The most effective outcomes were produced by the integration of Convolutional Neural Networks with additional factors like Age, Gender, BMI, Injury, Surgery, WOMAC score and KL-grade. Subsequently, it was combined with Gradient Boosted Machines.

Bonaretti et al., [113] presented the mean characteristics of the OAI Control and Incidence Cohort of the selected patients. All subjects in OA groups were monitored for the symptomatic progression of KL grades of 0 baselines. In WOMAC, the control group had a decrease of 0.1 over 36 months, suggesting a lack of development. The OA group's symptomatic progression had a change in WOMAC of 25, indicating a consistent development of the OA symptoms over a follow-up span of 36 months. The OA group symptomatic development was significantly higher in the theme age and BMI than in the control group (age: 56, BMI: 25, Mean change in WOMAC: -0.1, Mean baseline KL: 0) and (age: 59, BMI: 29, Mean change in WOMAC: -25, Mean baseline KL: 0)

Nguyen et al. [114] introduced a technique that includes two components: a) An innovative version of Siamese network and b) an original Deep SSL method. In their suggested method, the Siamese model emphasizes the medial and lateral aspects of the analyzed knee. They chose three architectures: GAP, SAM-VH, and SAM-HV based on their average BAs. The top option from these (i.e., SAMHV) has been chosen as the foundational model for SSL methods. Their reported findings indicate that their SAM architecture outperformed the Baseline SL model across all dataset configurations. In reality, their SAM-HV design outperformed the BAs Baseline by 9%. It seems that your message is incomplete. In the scenario of 500 samples per KL, the SAM-HV model outperformed the baseline model by 6%. The accuracy of their early detection OA system (which implies KL = 2) with 500 and 1000 marks per grade KL, was 58% and 74%, respectively

Yoo et al. [70] developed a scoring system and enhanced the ANN model utilizing indicators like gender, age, body mass index, education level, high blood pressure, moderate exercise, and knee discomfort. The scoring system and ANN forecasted radiographic knee OA (AUC 0.73 compared to 0.81, $p < 0.001$) and symptomatic knee OA demonstrated a strong discriminative capability in internal validation (AUC 0.88 vs. 0.94, $p < 0.001$). Every aspect of the scoring framework and ANN exhibited reduced ability in forecasting radiographic knee OA (AUC 0.62 compared to 0.67, $p < 0.001$) and symptomatic knee OA (AUC 0.7) during external validation.

For the OAI demographic, the scoring system forecasted radiographic and symptomatic knee osteoarthritis with AUCs of 0.62 and 0.70, respectively, and the ANN with the AUCs of 0.66 and 0.76, correspondingly.

IX. DIAGNOSIS :

Typical examination results include heat, compassion, edema, and waterlogging, as well as muscle loss close to the affected joints. Differential rheumatoid factor and the sedimentation rate of erythrocytes or C-reactive proteins are among the first laboratory tests. To treat viral or crystal-induced arthritis, suction of the joint may occasionally be necessary (in case of monoarticular presentations). Tests for baseline renal and hepatic function (for the purpose of selecting drugs)

An anti-cyclic citrullinated peptide antibody can have a positive predictive value and a higher specificity; less than 60% of patients with rheumatoid arthritis have this antibody [46].

X. SURGERY:

. Synovectomy: The injured lining of the joint is removed by surgery is performed on the knees, elbows, wrists, fingers, and hips [49].



Fig. 3. Arthroscopic synovectomy (removal of synovium damaging the joints by inserting a miniature camera) of wrist (B) Wrist joint diffuse synovectomy (C) Removal of synovium successively

Source: https://www.researchgate.net/figure/A-Arthroscopic-synovectomy-of-the-wrist-rheumatoid-arthritis-B-Intraoperative_fig1_273185482 (Accessed on 10 June 2020)

. **Repair of tendon:** The tendons around the joints will slacken or break due to tenderness and destruction of the joint and the joints around the dented joints are repaired.



Fig. 4. Ankle ligament reconstruction

Source: <https://murdochorthopaedic.com.au/our-surgeons/peter-ammon/procedures/ankle-arthroscopy-ankle-ligament-reconstruction/> (Accessed on 10 June 2020)

Fusion of joint: For the purpose of realignment or stabilization of the joint and relieving from the pain, the joints are fused.

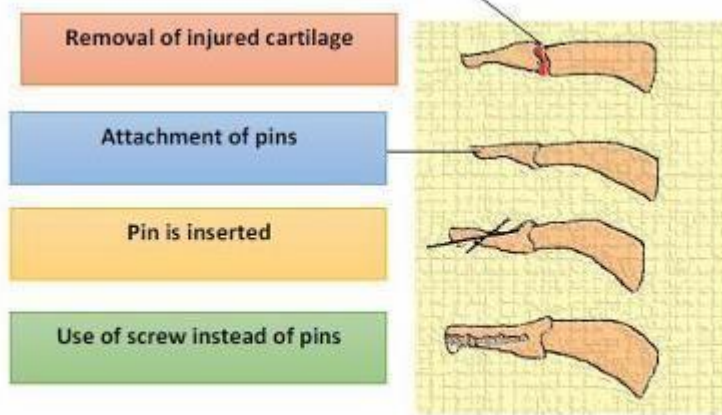


Fig. 5. Fusion of arthritic dip point in fingers

Source: <https://centralcoastortho.com/patient-education/finger-fracture-fixation/> (Accessed on 10 June 2020)

. Replacement of the total joint: The dented parts are removed from the joint and fake thing made of metal and plastic was inserted [50].



Fig. 6. Knee joint replacement

Source: <https://www.houstonhipandkneesurgeon.com/less-invasive-knee.html> (Accessed on 10 June 2020)

XI.TREATMENT:

Rheumatoid arthritis treatment necessitates the patient's understanding of the condition.

Three methods are used to treat rheumatoid arthritis: DMARDs, biologics, and intra-articular or oral (low dose) NSAIDs and glucocorticoids.

NSAIDs: They lessen joint pain and swelling without changing the course of the disease. Warning: Do not use on your own.

Steroids: They alleviate symptoms and slow down joint deterioration. Indication: For a brief duration, lesser dosages (bridge therapy) should be used.

[Oral doses of calcium and vitamin D: prevent bone demineralization].

DMARDs: Slow down the disease's progression and improve long-term forecasting.

Biologics: Target inflammatory cells, signaling molecules, cytokines, and joint destruction.

Table 1. List of DMARDs used to treat rheumatoid arthritis (47)

Sl. no	Drug	Dose
1	Sulfasalazine	2-3 g daily
2	Etanercept	25 mg twice/week or 50mg sc weekly
3	Methotrexate	15 mg/week
4	Adatumumab	40 mg (biweekly)
5	Cyclosporine	2.5-5 mg/day

First-line agents: Adalimumab, etanercept, infliximab IL-1 Antagonist:

Anakinra

Anti-Bcell antibody: Rituximab

Down-regulator of T-cell co-stimulation: Abatacept

Disadvantages: Risk of infection is more, tuberculosis may be reactivated [48)

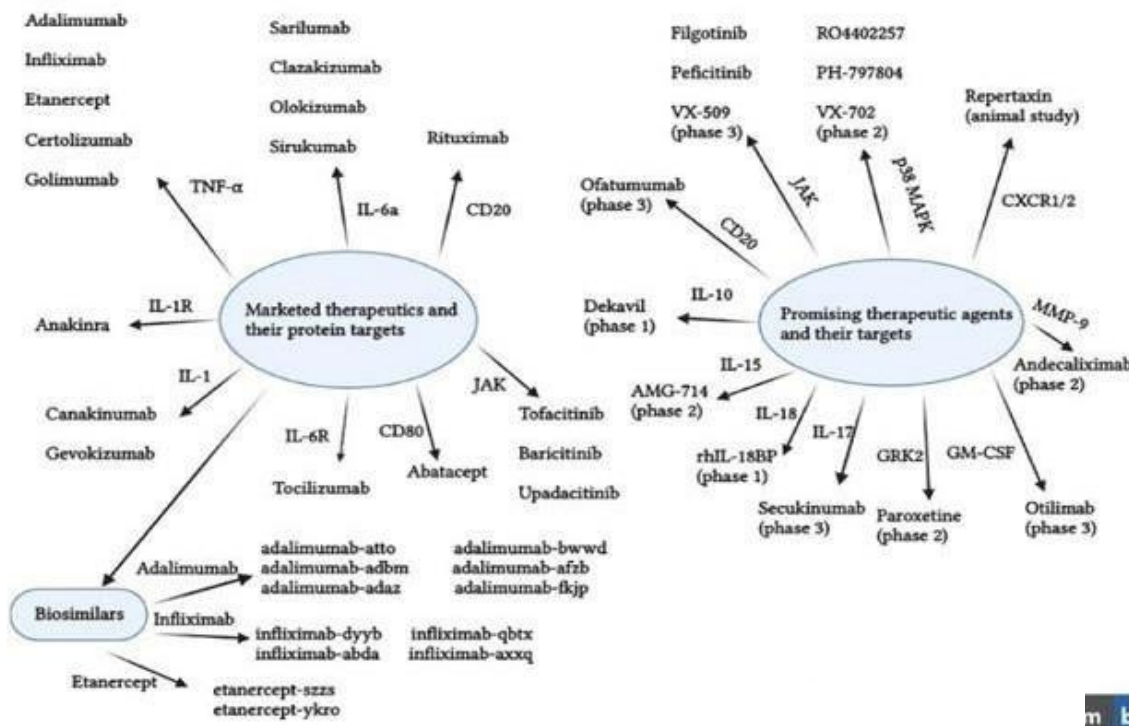
List of marketed product of drugs used in rheumatoid arthritis:

Sr.no	Brand name	drug	formulation	Drug class	reference
1	Otrexup	Methotrexate	Injection(sc)	Antimetabolites Antirheumatics Antipsoriatics	51
2	Celebrex	Celecoxib	Tablet	COX2 Inhibitor	52
3	Plaquenil	Hydrochloroquine	Tablet	Antirheumatics Antimalarial	53
4	Mobix G SPRAY	Meloxicam	Spray	NSAID	54
5	Humira	Adalimumab	Biologic	Antirhuematic TNF-a inhibitors	55
6	Acetemra	Tocilizumab	Injection(sc)	IL inhibitors	56
7	Arava	Leflunomide	Oral	DMARD Immunosuppressant	57
8	Remicad	Infliximab	Injection(IV)	Antirhuematic TNF-a Inhibitors	58
9	Orencia	Abatacept	Injection (IV)	Antirheumatic Immunosuppressant	59
10	norco	Acetaminophen hydrocodone	tablet	Narcotic analgesic combinations	60

XII. NEW PERSPECTIVES AND FUTURE DIRECTIONS IN THE TREATMENT OF RA:

Over the past few decades, RA treatment has improved patients' quality of life and results. The identification of many routes in the pathophysiology of RA has made this possible. However,

Uncertainty remains regarding the underlying mechanisms of inflammation and the pharmacological effects of therapeutic agents, resulting in unmet requirements in managing RA. This includes understanding how different medicines have equivalent efficacy and why some individuals grow less responsive over time. Detecting pre-RA and initiating aggressive therapy, as well as enhancing the effectiveness and safety of new drugs, particularly JAK inhibitors [123,119]. Several strategies to enhance RA therapy are presently being investigated in different settings. Experiments are used. To achieve full remission of RA, researchers are exploring novel treatment targets and evaluating promising medicines. Figure (122,118)] summarizes the current and future of targeted therapy



.Figure . Status and future targeted therapies in RA. AMG, human monoclonal antibody; CD20, membrane-embedded surface molecule; CXCR-,chemokine receptor; IL, interleukin; CD80, ligand for the protein CD28; JAK, Janus kinase; MAPK,mitogen-activated protein kinases; MMP, matrix, metalloproteinase; TNF-, tumor necrosis factor alpha.

Huang et al. (2021) updated and considered complex information about small molecular metabolite targets (prostaglandins, thromboxane A2, leukotriene B4 receptor, platelet activating factor, cannabinoid receptors, inducible nitric oxide, etc.), epigenetic targets (DNA methylation, RNA methylation, histone modification, etc.), and other protein targets (p38 mitogen-activated protein kinase, complex G protein-coupled receptor kinase 2, granulocyte-macrophage mesenchymal stem cells (MSCs) have the potential to develop into new tissues such as bone and cartilage and have been shown to decrease T cell activation in vitro, making them a prospective therapeutic option. Treatment with MSCs has been demonstrated to reduce proinflammatory response and improve RA symptoms by lowering blood levels of IL-1, IL-6, IL-8, and TNF-[120]. Toll-like receptor 4 has a function in RA etiology by increasing joint inflammation. Therapeutic drugs that target this receptor or its ligands, including heat-shock protein crystalline or tenascin C, can be optimized [120]. Numerous current investigations can lead to major improvements for RA patients by identifying novel molecular targets and therapies. And novel strategies for mitigating negative effects. A tailored strategy combining genetic studies and evidence-based treatment has the potential to cure incurable diseases [121].

CONCLUSION

Rheumatoid arthritis (RA) is a debilitating chronic inflammatory disease that significantly impairs the quality of life of affected individuals, primarily the elderly population and women. This review has provided an in-depth examination of the molecular mechanisms underlying RA, including the crucial role of major histocompatibility complex molecules and dependent T-cells in triggering and sustaining the autoimmune response. The current treatment options and management strategies for RA have also been comprehensively reviewed, highlighting the importance of a multi-faceted approach to mitigate the disease's systemic consequences and improve patient outcomes.

The findings of this review underscore the complex interplay between autoimmune cells, joint inflammation, and tissue destruction in RA, which necessitates a comprehensive treatment strategy that targets multiple pathways. The significant morbidity and mortality associated with RA, including the increased risk of heart conditions and pulmonary problems, emphasize the need for early diagnosis, timely intervention, and ongoing management to prevent long-term disability and reduce the risk of comorbidities.

Overall, this review contributes to the existing body of knowledge on RA by providing a detailed understanding of the disease's molecular mechanisms and highlighting the importance of a multifaceted approach to treatment and management. The insights gained from this study can inform the development of more effective therapeutic strategies, improve patient outcomes, and ultimately reduce the significant burden of RA on individuals, healthcare systems, and society as a whole. Future research should continue to explore the molecular mechanisms underlying RA and investigate novel therapeutic approaches to improve the management and treatment of this debilitating disease.

References:

1. Alope C, Ibiama UA, Orji OU, Ugwuja EI Ezeani NN, Aja PM, Obasi NA. Antiarthritic potentials of ethanol and aqueous extracts of stem bark of *Cleistopholis patens* on complete Freund's adjuvant-induced rheumatoid arthritis in rats. *Journal of Ayurveda and Integrative Medicine*; 2019.
2. Girdler SJ, Ye I, Tang R, Kirschner N Altering the natural history of rheumatoid arthritis: The role of immunotherapy and biologics in orthopaedic care. *Journal of Orthopaedics*. 2020;17:17-21.
3. Esposito AJ, Chu SG, Madan R, Doyle TJ, Dellaripa PF. Thoracic manifestations of rheumatoid arthritis. *Clinics in Chest Medicine*. 2019;40(3):545-60.
4. Jayashree S, Nirekshana K, Guha G, Bhakta-Guha D. Cancer chemotherapeutics in rheumatoid arthritis: A convoluted connection. *Biomedicine & Pharmacotherapy*. 2018;102:894-911.
5. Hoxha M. A systematic review on the role of eicosanoid pathways in rheumatoid arthritis. *Advances in Medical Sciences*. 2018;63(1):22-9.
6. Tanaka S. Emerging anti-osteoclast therapy for rheumatoid arthritis. *Journal of Orthopaedic Science*. 2018;23(5):717-21.
7. Wang X, Fang G, Yang Y, Pang Y. The newly discovered natural compounds against rheumatoid arthritis-an overview. *Phytochemistry Letters*. 2019;34:50-8.
8. Syed A, Devi VK. Potential of targeted drug delivery systems in treatment of rheumatoid arthritis. *Journal of Drug Delivery Science and Technology*
- 9] M. Roques, F. Tanchoux, L. Calvière, L. Cuinat, V. Lubrano, E. Uro-Coste, C. Cognard, V. Larrue, F. Bonneville, Mri with dwi helps in depicting rheumatoid meningitis, *J. Neuroradiol*. 41 (2014) 275–277
- 10) Australian Bureau of Statistics, National health survey: first results, [https:// www.abs.gov.au/ausstats/](https://www.abs.gov.au/ausstats/), 2020. (Accessed 4 May 2020).
- 11] Australian Institute of Health and Welfare, Arthritis.
- 12)] J. Van den Hoek, H. Boshuizen, L. Roorda, G. Tijhuis, M. Nurmohamed, G. van den Bos, J. Dekker, Mortality in patients with rheumatoid arthritis: a 15-year prospective cohort study, *Rheumatol. Int*. 37 (2017) 487–493.
- 13)] S.A.A. Shah, K. Yahya, G. Mubashar, A. Bais, Quantification and visualization of mri cartilage of the knee: a simplified approach, in: 2010 6th International Conference on Emerging Technologies (ICET), IEEE, 2010, pp. 175–180.
- 14)] R.I. Doewes, L. Gangadhar, S. Subburaj, An overview on stress neurobiology: fundamental concepts and its consequences, *Neurosci. Inform*. 1 (2021) 100011
- 15) A. Sujith, G.S. Sajja, V. Mahalakshmi, S. Nuhmani, B. Prasanalakshmi, Systematic review of smart health monitoring using deep learning and artificial intelligence, *Neurosci. Inform*. 2 (2022) 100028
- 16)] M. Hügle, P. Omoumi, J.M. van Laar, J. Boedecker, T. Hügle, Applied machine learning and artificial intelligence in rheumatology, *Rheumatol. Adv. Pract*. 4 (2020) rkaa005
- 17)] R.M. Loureiro, J. Collin, D.V. Sumi, L.C. Araújo, R.W. Murakoshi, R.L.E. Gomes, M.M. Daniel, Postoperative ct findings of orthognathic surgery and its complications: a guide for radiologists, *J. Neuroradiol*. (2021).
- 18)] A. Tiulpin, J. Thevenot, E. Rahtu, S. Saarakkala, A novel method for automatic localization of joint area on knee plain radiographs, in: *Scandinavian Conference on Image Analysis*, Springer, 2017, pp. 290–301
- 19)] K.J. Kim, I. Tagkopoulos, Application of machine learning in rheumatic disease research, *Korean J. Int. Med*. 34 (2019) 708.
- 20)] U. Nadeem, S.A.A. Shah, M. Bennamoun, R. Togneri, F. Sohel, Real time surveillance for low resolution and limited-data scenarios: an image set classification approach, *Inf. Sci*. (2021)
- 21)] S.A. Shah, U. Nadeem, M. Bennamoun, F. Sohel, R. Togneri, Efficient image set classification using linear regression based image reconstruction, in: *Proceedings of the IEEE Conference on Computer Vision and Pattern Recognition Workshops*, 2017, pp. 99–108.

22)] S.D. Pande, P.P. Jadhav, R. Joshi, A.D. Sawant, V. Muddebihalkar, S. Rathod, M.N.

Gurav, S. Das, Digitization of handwritten Devanagari text using cnn transfer learning – a better customer service support, *Neurosci. Inform. 2* (2022)

100016.

23)] B. Stoel, Use of artificial intelligence in imaging in rheumatology–current status and future perspectives, *RMD Open 6* (2020) e001063

24)] A. Jamshidi, J.P. Pelletier, J. Martel-Pelletier, Machine-learning-based patientspecific prediction models for knee osteoarthritis, *Nat. Rev. Rheumatol. 15*

(2019) 49–60

25)] C. Kokkoti, S. Moustakidis, E. Papageorgiou, G. Giakas, D. Tsaopoulos, Machine learning in knee osteoarthritis: a review, *Osteoarthr. Cartil. Open 2* (2020)

100069.

26) Firestein, G.S.; McInnes, I.B. Immunopathogenesis of rheumatoid arthritis. *Immunity 2017*, *46*, 183–196. [CrossRef]

27) Curran, A.M.; Naik, P.; Giles, J.T.; Darrah, E. PAD enzymes in rheumatoid arthritis: Pathogenic effectors and autoimmune targets. *Nat. Rev. Rheumatol. 2020*, *16*, 301–315. [CrossRef]

28). Scherer, H.U.; Häupl, T.; Burmester, G.R. The etiology of rheumatoid arthritis. *J. Autoimmun. 2020*, *110*, 102400. [CrossRef]

29). Damerau, A.; Gaber, T. Modeling rheumatoid arthritis in vitro: From experimental feasibility to physiological proximity. *Int. J. Mol. Sci. 2020*, *21*, 7916. [CrossRef] [PubMed]

30). van Drongelen, V.; Holoshitz, J. HLA-disease associations in rheumatoid arthritis. *Rheum. Dis. Clin. North Am. 2017*, *43*, 363–376.

[CrossRef]

31). Frauwirth, K.A.; Thompson, C.B. Activation and inhibition of lymphocytes by costimulation. *J. Clin. Investig. 2002*, *109*, 295–299.

[CrossRef] [PubMed]

32). Isaacs, J.D. Therapeutic T-cell manipulation in rheumatoid arthritis: Past, present and future. *Rheumatology 2008*, *47*, 1461–1468.

[CrossRef] [PubMed]

33) Stavnezer, J.; Guikema, J.E.J.; Schrader, C.E. Mechanism and regulation of class switch recombination. *Annu. Rev. Immunol. 2008*,

26, 261–292. [CrossRef]

34) Ingegnoli, F.; Castelli, R.; Gualtierotti, R. Rheumatoid factors: Clinical applications. *Dis. Markers 2013*, *35*, 727–734. [CrossRef]

35) Yu, H.C.; Lu, M.C. The roles of anti-citrullinated protein antibodies in the immunopathogenesis of rheumatoid arthritis. *Tzu-Chi Med. J. 2019*, *31*, 5–10. [CrossRef]

36) K.J. Kim, I. Tagkopoulos, Application of machine learning in rheumatic disease research, *Korean J. Int. Med. 34* (2019) 708.

37)] M. Kourilovitch, C. Galarza-Maldonado, E. Ortiz-Prado, Diagnosis and classification of rheumatoid arthritis, *J. Autoimmun. 48* (2014) 26–30

38)] A. Tiulpin, J. Thevenot, E. Rahtu, S. Saarakkala, A novel method for automatic

localization of joint area on knee plain radiographs, in: *Scandinavian Conference on Image Analysis*, Springer, 2017, pp. 290–301.

39)] A. Tiulpin, J. Thevenot, E. Rahtu, S. Saarakkala, A novel method for automatic

localization of joint area on knee plain radiographs, in: *Scandinavian Conference on Image Analysis*, Springer, 2017, pp. 290–301.

40)] S.S. Gornale, P.U. Patravali, R.R. Manza, Computer assisted analysis and systemization of knee osteoarthritis using digital x-ray images, in: *Proceedings of 2nd International Conference on Cognitive Knowledge Engineering (ICKE)*, 2016, pp. 207–212.

- 41)] S.S. Gornale, P.U. Patravali, R.R. Manza, Computer assisted analysis and systemization of knee osteoarthritis using digital x-ray images, in: Proceedings of 2nd International Conference on Cognitive Knowledge Engineering (ICKE), 2016, pp. 207–212.
- 42)] A. Tiulpin, I. Melekhov, S. Saarakkala, Kneel: knee anatomical landmark localization using hourglass networks, in: Proceedings of the IEEE International Conference on Computer Vision Workshops, 2019
- 43)] A. Chattopadhyay, M. Maitra, Mri-based brain tumor image detection using cnn based deep learning method, *Neurosci. Inform.* (2022) 100060
- 44)] J. Yoo, M.K. Lim, C. Ihm, E.S. Choi, M.S. Kang, A study on prediction of rheumatoid arthritis using machine learning, *Int. J. Appl. Eng. Res.* 12 (2017) 9858–9862
- 45) Martins P, Fonseca JE. How to investigate: Pre-clinical rheumatoid arthritis. *Best Practice & Research Clinical Rheumatology.* 2019;101438.
- 46) Birch JT, Bhattacharya S. Emerging trends in diagnosis and treatment of rheumatoid arthritis. *Primary Care: Clinics in Office Practice.* 2010;37(4):779-92
- 47) Margaretten M, Julian L, Katz P, Yelin E. Depression in patients with rheumatoid arthritis: Description, causes and mechanisms. *International Journal of Clinical Rheumatology.* 2011;6(6):617
- 48) Majithia V, Geraci SA. Rheumatoid arthritis: Diagnosis and management. *The American Journal of Medicine* 2007;120(11):936-9
- 49) Woo SJ, Park MJ. Current concept of surgical management for rheumatoid arthritis of the wrist. *Journal of the Korean Society for Surgery of the Hand.* 2013;18(4):196-205.
- 50) Vivek Sood. Types of knee surgery for arthritis treatment, *Arthritis-Health.* Arthritis Health. 2013;1–5.
Available:<https://www.arthritishealth.com/surgery/knee-surgery/typesknee-surgery-arthritis-treatment>
- 51) Otrexup.com. Home: Otrexup (methotrexate) injection for subcutaneous use; 2009. [Online] Available:<https://www.otrexup.com/>
- 52). <https://www.facebook.com/Drugscom> Celebrex. *Drugs.com*; 2019. [Online] Available:<https://www.drugs.com/celebrex.html> (Accessed 5 November 2019)
- 53). *Webmd.com. Drugs & Medications*; 2019. [Online] Available:<https://www.webmd.com/drugs/2/drug-6986/plaquenil-oral/details> (Accessed 7 December 2019)
- 54). *TabletWise.com. Mobix G Spray - Uses, side-effects, reviews and precautions - Cipla - TabletWise - India.* Tabletwise;2016. [Online]
- 55) *Humira.com. HUMIRA® (adalimumab). A Biologic Treatment Option*; 2013. [Online] Available:<https://www.humira.com/> (Accessed 7 December 2019)
- 56). *RxList. Actemra*; 2019. [Online] Available:<https://www.rxlist.com/actemradrug.htm> (Accessed 7 December 2019)
- 57). *Medscape.com. Arava (leflunomide) dosing, indications, interactions, adverse effects and more*; 2019. [Online] Available:<https://reference.medscape.com/drug/arava-leflunomide-343203> (Accessed 7 December 2019)
- 58). *Official Website for REMICADE® (infliximab). Home*; 2016. [Online] Available:<https://www.remicade.com/>
- 59). *Orencia.com. ORENCIA (abatacept)*; 2019. [Online] Available:<https://www.orencia.com/> (Accessed 15 October 2019)
- 60) <https://www.facebook.com/Drugscom>. List of Rheumatoid Arthritis Medications (218 Compared) - *Drugs.com*; 2019. [Online] Available:<https://www.drugs.com/condition/rheumatoid-arthritis.html> (Accessed 6 May 2019)
- 61) K.J. Kim, I. Tagkopoulos, Application of machine learning in rheumatic disease research, *Korean J. Int. Med.* 34 (2019) 708.
- 62) M. Kuhn, K. Johnson, *Applied Predictive Modeling*, vol. 26, Springer, 2013.

- 63) M. Hügle, P. Omoumi, J.M. van Laar, J. Boedecker, T. Hügle, Applied machine learning and artificial intelligence in rheumatology, *Rheumatol. Adv. Pract.* 4 (2020) rkaa005
- 64) S.M. Zhou, F. Fernandez-Gutierrez, J. Kennedy, R. Cooksey, M. Atkinson, S. Denaxas, S. Siebert, W.G. Dixon, T.W. O'Neill, E. Choy, et al., Defining disease phenotypes in primary care electronic health records by a machine learning approach: a case study in identifying rheumatoid arthritis, *PLoS ONE* 11 (2016) e0154515.
- 65) T.K. Ho, Random decision forests, in: *Proceedings of 3rd International Conference on Document Analysis and Recognition, IEEE, 1995*, pp. 278–282.
- 66) S.B. Maind, P. Wankar, et al., Research paper on basic of artificial neural network, *Int. J. Recent Innov. Trends Comput. Commun.* 2 (2014) 96–100
- 67) O.I. Abiodun, A. Jantan, A.E. Omolara, K.V. Dada, N.A. Mohamed, H. Arshad, State-of-the-art in artificial neural network applications: a survey, *Heliyon* 4 (2018) e00938.
- 68) J. MacQueen, et al., Some methods for classification and analysis of multivariate observations, in: *Proceedings of the Fifth Berkeley Symposium on Mathematical Statistics and Probability, Oakland, CA, USA, 1967*, pp. 281–297
- 69) U.V. Singh, E. Gupta, T. Choudhury, Detection of rheumatoid arthritis using machine learning, in: *2019 International Conference on Computational Intelligence and Knowledge Economy (ICCIKE), IEEE, 2019*, pp. 25–29.
- 70) J. Yoo, M.K. Lim, C. Ihm, E.S. Choi, M.S. Kang, A study on prediction of rheumatoid arthritis using machine learning, *Int. J. Appl. Eng. Res.* 12 (2017) 9858–9862
- 71) R.S. Sutton, A.G. Barto, *Reinforcement Learning: An Introduction*, MIT Press, 2018
- 72) S.A.A. Shah, M. Bennamoun, F. Boussaid, Iterative deep learning for image set based face and object recognition, *Neurocomputing* 174 (2016) 866–874.
- 73) B. Stoel, Use of artificial intelligence in imaging in rheumatology—current status and future perspectives, *RMD Open* 6 (2020) e001063.
- 74) K. O'Shea, R. Nash, An introduction to convolutional neural networks, arXiv preprint, arXiv:1511.08458, 2015.
- 75) I.J. Goodfellow, J. Pouget-Abadie, M. Mirza, B. Xu, D. Warde-Farley, S. Ozair, A. Courville, Y. Bengio, Generative adversarial networks, arXiv preprint, arXiv: 1406.2661, 2014.)
- 76) S. Khan, H. Rahmani, S.A.A. Shah, M. Bennamoun, A guide to convolutional neural networks for computer vision, in: *Synthesis Lectures on Computer Vision*, vol. 8, 2018, pp. 1–207
- 77) J. Gutiérrez-Martínez, C. Pineda, H. Sandoval, A. Bernal-González, Computeraided diagnosis in rheumatic diseases using ultrasound: an overview, *Clin.Rheumatol.* (2020) 1–13
- 78) J. Long, E. Shelhamer, T. Darrell, Fully convolutional networks for semantic segmentation, in: *Proceedings of the IEEE Conference on Computer Vision and Pattern Recognition, 2015*, pp. 3431– 3440.
- 79) B. Norman, V. Pedoia, A. Noworolski, T.M. Link, S. Majumdar, Applying densely connected convolutional neural networks for staging osteoarthritis severity from plain radiographs, *J. Digit. Imaging* 32 (2019) 471–477.
- 80) C.E. von Schacky, J.H. Sohn, F. Liu, E. Ozhinsky, P.M. Jungmann, L. Nardo, M. Posadzy, S.C. Foreman, M.C. Nevitt, T.M. Link, et al., Development and validation of a multitask deep learning model for severity grading of hip osteoarthritis features on radiographs, *Radiology* 295 (2020) 136–145.
- 81) T.Y. Lin, P. Goyal, R. Girshick, K. He, P. Dollár, Focal loss for dense object detection, in: *Proceedings of the IEEE International Conference on Computer Vision, 2017*, pp. 2980–2988.

- 82) B. Liu, J. Luo, H. Huang, Toward automatic quantification of knee osteoarthritis severity using improved faster r-cnn, *Int. J. Comput. Assisted Radiol. Surg.* 15 (2020) 457–466.
- 83) N.N. Khanna, A.D. Jamthikar, D. Gupta, M. Piga, L. Saba, C. Carcassi, A.A. Giannopoulos, A. Nicolaidis, J.R. Laird, H.S. Suri, et al., Rheumatoid arthritis: atherosclerosis imaging and cardiovascular risk assessment using machine and deep learning–based tissue characterization, *Curr. Atheroscler. Rep.* 21 (2019) 7.
- 84) K. Üreten, H. Erbay, H.H. Maras, , Detection of rheumatoid arthritis from hand radiographs using a convolutional neural network, *Clin. Rheumatol.* 39 (2020) 969–974.
- 85) G.J. Fent, J.P. Greenwood, S. Plein, M.H. Buch, The role of noninvasive cardiovascular imaging in the assessment of cardiovascular risk in rheumatoid arthritis: where we are and where we need to be, *Ann. Rheum. Dis.* 76 (2017) 1169–1175.
- 86) K.J. Kim, I. Tagkopoulos, Application of machine learning in rheumatic disease research, *Korean J. Int. Med.* 34 (2019) 708.
- 87) J.M. Lezcano-Valverde, F. Salazar, L. León, E. Toledano, J.A. Jover, B. FernandezGutierrez, E. Soudah, I. González-Álvaro, L. Abasolo, L. Rodriguez-Rodriguez, Development and validation of a multivariate predictive model for rheumatoid arthritis mortality using a machine learning approach, *Sci. Rep.* 7 (2017) 1–10.
- 88) S. Murakami, K. Hatano, J. Tan, H. Kim, T. Aoki, Automatic identification of bone erosions in rheumatoid arthritis from hand radiographs based on deep convolutional neural network, *Multimed. Tools Appl.* 77 (2018) 10921–10937
- 89) D.E. Orange, P. Agius, E.F. DiCarlo, N. Robine, H. Geiger, J. Szymonifka, M. McNamara, R. Cummings, K.M. Andersen, S. Mirza, et al., Identification of three rheumatoid arthritis disease subtypes by machine learning integration of synovial histologic features and RNA sequencing data, *Arthritis Rheumatol.* 70 (2018) 690–701.
- 90) U.V. Singh, E. Gupta, T. Choudhury, Detection of rheumatoid arthritis using machine learning, in: 2019 International Conference on Computational Intelligence and Knowledge Economy (ICCIKE), IEEE, 2019, pp. 25–29.
- 91) K. Üreten, H. Erbay, H.H. Maras, , Detection of rheumatoid arthritis from hand radiographs using a convolutional neural network, *Clin. Rheumatol.* 39 (2020) 969–974
- 92) J. Thomson, T. O'Neill, D. Felson, T. Cootes, Automated shape and texture analysis for detection of osteoarthritis from radiographs of the knee, in: International Conference on Medical Image Computing and Computer-Assisted Intervention, Springer, 2015, pp. 127–134.
- 93) S.S. Gornale, P.U. Patravali, R.R. Manza, Computer assisted analysis and systemization of knee osteoarthritis using digital x-ray images, in: Proceedings of 2nd International Conference on Cognitive Knowledge Engineering (ICKE), 2016, pp. 207–212.
- 94) S.S. Gornale, P.U. Patravali, R.R. Manza, Detection of osteoarthritis using knee x-ray image analyses: a machine vision based approach, *Int. J. Comput. Appl.* 145 (2016).
- 95) S.S. Gornale, P.U. Patravali, K.S. Marathe, P.S. Hiremath, Determination of osteoarthritis using histogram of oriented gradients and multiclass svm, *Int. J. Image Graph. Signal Process.* 9 (2017)
- 96) A. Tiulpin, J. Thevenot, E. Rahtu, S. Saarakkala, A novel method for automatic localization of joint area on knee plain radiographs, in: Scandinavian Conference on Image Ana 97)A. Tiulpin, J. Thevenot, E. Rahtu, P. Lehenkari, S. Saarakkala, Automatic knee osteoarthritis diagnosis from plain radiographs: a deep learning-based approach,

Sci. Rep. 8 (2018) 1–10. lysis, Springer, 2017, pp. 290–301

98) A. Tiulpin, I. Melekhov, S. Saarakkala, Kneel: knee anatomical landmark localization using hourglass networks, in: Proceedings of the IEEE International Conference on Computer Vision Workshops, 2019

99) J. Antony, K. McGuinness, K. Moran, N.E. O'Connor, Automatic detection of knee joints and quantification of knee osteoarthritis severity using convolutional

neural networks, in: International Conference on Machine Learning and Data Mining in Pattern Recognition, Springer, 2017, pp. 376–390.

100) A.A. Tolpadi, J.J. Lee, V. Pedoia, S. Majumdar, Deep learning predicts total knee replacement from magnetic resonance images, Sci. Rep. 10 (2020) 1–12.

101) C. Wang, Z. Peng, Design and implementation of an object detection system using faster r-cnn, in: 2019 International Conference on Robots & Intelligent System (ICRIS), IEEE, 2019, pp. 204–206.

102)] L. Shamir, S.M. Ling, W. Scott, M. Hochberg, L. Ferrucci, I.G. Goldberg, Early detection of radiographic knee osteoarthritis using computer-aided analysis, Osteoarthr. Cartil. 17 (2009) 1307–1312.

103) J. Abedin, J. Antony, K. McGuinness, K. Moran, N.E. O'Connor, D. RebholzSchuhmann, J. Newell, Predicting knee osteoarthritis severity: comparative

modeling based on patient's data and plain x-ray images, Sci. Rep. 9 (2019) 1–11.

104) P. Chen, L. Gao, X. Shi, K. Allen, L. Yang, Fully automatic knee osteoarthritis severity grading using deep neural networks with a novel ordinal loss, Comput. Med. Imaging Graph. 75 (2019) 84–92.

105)] J. Antony, K. McGuinness, N.E. O'Connor, K. Moran, Quantifying radiographic knee osteoarthritis severity using deep convolutional neural networks, in:

2016 23rd International Conference on Pattern Recognition (ICPR), IEEE, 2016,

pp. 1195–1200.

106) H. Hoang Nguyen, S. Saarakkala, M. Blaschko, A. Tiulpin, Semixup: in- and outof-manifold regularization for deep semi-supervised knee osteoarthritis severity grading from plain radiographs, arXiv:2003.01944, 2020.

107) K.A. Thomas, Ł. Kidzinski, ´ E. Halilaj, S.L. Fleming, G.R. Venkataraman, E.H. Oei,

G.E. Gold, S.L. Delp, Automated classification of radiographic knee osteoarthritis severity using deep neural networks, Radiol. Artif. Intell. 2 (2020) e190065.

108) S.S. Gornale, P.U. Patravali, R.R. Manza, Computer assisted analysis and systemization of knee osteoarthritis using digital x-ray images, in: Proceedings of 2nd International Conference on Cognitive Knowledge Engineering (ICKE), 2016, pp. 207–212.

109) .Zvaifler, N. J., Steinman, R. M., Kaplan, G., Lau, L. L. & Rivelis, M. Identification of immunostimulatory dendritic cells in the synovial effusions of patients with rheumatoid arthritis. J. Clin. Invest. 76, 789–800 (1985).

110) B. Norgeot, B.S. Glicksberg, L. Trupin, D. Lituiev, M. Gianfrancesco, B. Oskotsky,

G. Schmajuk, J. Yazdany, A.J. Butte, Assessment of a deep learning model based on electronic health record data to forecast clinical outcomes in patients with rheumatoid arthritis, JAMA Netw. Open 2 (2019) e190606.

111) M.D. Li, K. Chang, B. Bearce, C.Y. Chang, A.J. Huang, J.P. Campbell, J.M. Brown, P. Singh, K.V. Hoebel, D. Erdogmus ~ , , et al., Siamese neural networks for continuous disease severity evaluation and change detection in medical imaging, npj Digit.

Med. 3 (2020) 1–9.

112) A. Tiulpin, S. Saarakkala, Automatic grading of individual knee osteoarthritis

features in plain radiographs using deep convolutional neural networks, Diagnostics 10 (2020) 932.

113) S. Bonaretti, G.E. Gold, G.S. Beaupre, pykneer: an image analysis workflow for open and reproducible research on femoral knee cartilage, PLoS ONE 15 (2020) e0226501

- 114) H.H. Nguyen, S. Saarakkala, M.B. Blaschko, A. Tiulpin, Annotation-efficient deep semi-supervised learning for automatic knee osteoarthritis severity diagnosis from plain radiographs, in: Online Proceedings Medical Imaging Meets NeurIPS Workshop 2020, NeurIPS, 2020
- 115) M. Subramoniam, A non-invasive method for analysis of arthritis inflammations by using image segmentation algorithm, in: 2015 International Conference on Circuits, Power and Computing Technologies [ICCPCT-2015], IEEE, 2015, pp. 1–4.
- 116) J. Tang, Z. Jin, X. Zhou, H. Chu, J. Yuan, M. Wu, Q. Cheng, X. Wang, Grading of rheumatoid arthritis on ultrasound images with deep convolutional neural network, in: 2018 IEEE International Ultrasonics Symposium (IUS), IEEE, 2018, pp. 1–4.
- 117) R. Hemalatha, V. Vijaybaskar, T. Thamizhvani, Automatic localization of anatomical regions in medical ultrasound images of rheumatoid arthritis using deep learning, Proc. Inst. Mech. Eng., H J. Eng. Med. 233 (2019) 657–667
- 118) S.D.H. Dang, L. Allison, Using deep learning to assign rheumatoid arthritis scores, in: 2020 IEEE 21st International Conference on Information Reuse and Integration for Data Science (IRI), IEEE, 2020, pp. 399–402
- 119) Huang, J.; Fu, X.; Chen, X.; Li, Z.; Huang, Y.; Liang, C. Promising therapeutic targets for treatment of rheumatoid arthritis. Front. Immunol. 2021, 12, 2716. [CrossRef]
- 120) Smolen, J.S.; Aletaha, D.; Barton, A.; Burmester, G.R.; Emery, P.; Firestein, G.S.; Kavanaugh, A.; McInnes, I.B.; Solomon, D.H.; Strand, V.; et al. Rheumatoid arthritis. Nat. Rev. Dis. Prim. 2018, 4, 1–23. [CrossRef] [PubMed]
- 121) Lin, Y.J.; Anzaghe, M.; Schülke, S. Update on the pathomechanism, diagnosis, and treatment options for rheumatoid arthritis. Cells 2020, 9, 880. [CrossRef] [PubMed]
- 122). Köhler, B.M.; Günther, J.; Kaudewitz, D.; Lorenz, H.M. Current therapeutic options in the treatment of rheumatoid arthritis. J. Clin. Med. 2019, 8, 938. [CrossRef] [PubMed]
- 123) Guo, Q.; Wang, Y.; Xu, D.; Nossent, J.; Pavlos, N.J.; Xu, J. Rheumatoid arthritis: Pathological mechanisms and modern pharmacologic therapies. Bone Res. 2018, 6, 1–15. [CrossRef] [PubMed]
- 124) Smolen, J.S.; Aletaha, D.; McInnes, I.B. Rheumatoid arthritis. Lancet 2016, 388, 2023–2038. [CrossRef]
- 125) Journal of Pharmaceutical Research International 32(12): 18-32, 2020; Article no.JPRI.58826
- ISSN: 2456-9119 (Past name: British Journal of Pharmaceutical Research, Past ISSN: 2231-2919, NLM ID: 101631759)